4. RESULTS

4.1 Bioinformatics analysis

Using the whole protein sequence of *Saccharomyces cerevisiae* SUMO (SMT3) as the query sequence, BLASTp search (http://www.broadinstitute.org/) was performed against *Magnaporthe oryzae* genome and a single copy of *SUMO* gene was identified (MGG_05737) (MoSUMO hereafter) with 53% identity at amino acid level. MoSUMO is a 330bp nucleotide sequence containing a single intron. The MoSUMO protein is highly conserved from yeast to humans and in plants as well. The multiple sequence alignment of MoSUMO with yeast, fungi, plants and human SUMO revealed that these proteins show an overall sequence similarity including the conserved diglycine motif, critical for SUMO conjugation, which is cleaved off by the desumoylating enzyme to produce the mature Gly-Gly carboxy terminus (Figure 6A). Furthermore, it also shared similarity at Lys residue lying within a sumoylation consensus site which indicates that MoSUMO has the potential to form poly-SUMO chains. The phylogenetic tree constructed using Neighbour-joining method, revealed that *MoSUMO* is closely related to *Colleotrichum fioroniae*, *Fusarium oxysporumn* and *Neurospora crassa* showing 82%, 81% and 78% identity respectively (Figure 6B).

Figure 6: *In silico* analysis of MoSUMO protein of *Magnaporthe oryzae* and phylogenetic analysis

A. Sequence alignment of the MoSUMO (MGG_05737) with SUMO of human, plant and *S. cerevisiae*, *S. pombe, C. albicans, N. crassa, F. oxysporum, C. fioroniae* with MUSCLE program. The conserved diglycine (GG) residue are highlighted in red. Lysine residue lying within sumoylation consensus site highlighted in blue.

B. Phylogram depicting the relationship between the human, yeast, and fungal SUMO. The phylogenetic tree was created using neighbor-joining method. Numbers at nodes represent bootstrap confidence values.

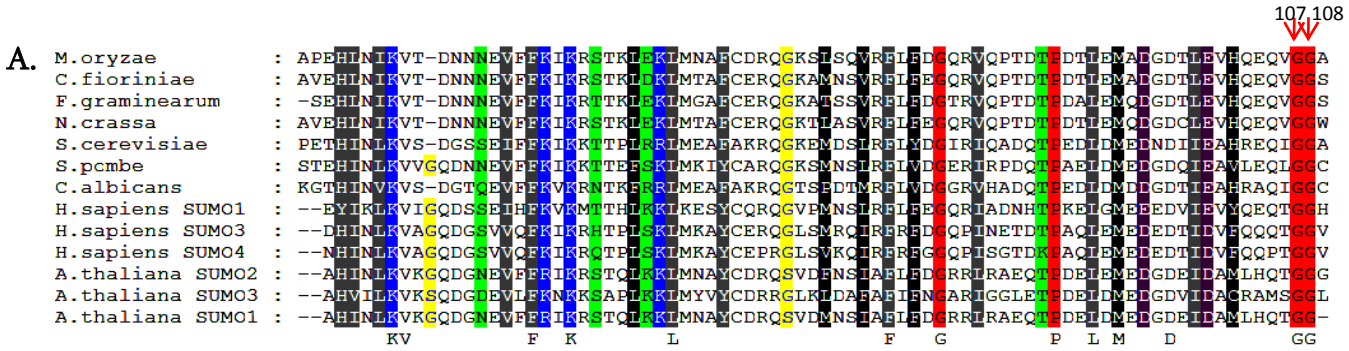
A.
107 108
M.oryzae : APEHINIKVT-DNNNEVFFKIKRSTKLEKLMNAFCDRQGKSLSQVRFLFDGQRVQPTDTPDTLEMADGDTLEVFQEQVGGA
C.fioriniae : AVEHINIKVT-DNNNEVFFKIKRSTKLEKLMTAFCERQGKAMNSVRFLFEGQRVQPTDTPDTLEMADGDTLEVFQEQVGGS
F.graminearum : -SEHINIKVT-DNNNEVFFKIKRTTKLEKLMGAFCERQGKATSSVRFLFDGTRVQPTDTPDAIEMQDGDTLEVFQEQVGGS
N.crassa : AVEHINIKVT-DNNNEVFFKIKRSTKLEKLMTAFCERQGKTLASVRFLFEGQRVQPTDTPDTLEMQDGDCLEVHQEQVGGW
S.cerevisiae : PETHINLKVS-DGSSEIFFKIKKTTPLRRLMEAFAKRQGKEMDSLRFLYDGIRIQADQTPEDLDMEDNDIIDAFREQIGGA
S.pombe : STEHINLKVVGQDNNEVFFKIKKTTPLSKLMKIYCARQGKSMNSLRFLYDGERIRPDQTPAELDMEDGDQIDAVLEQLGGC
C.albicans : KGTHINVKVS-DGTQEVFFKVKRNTKLRRLMEAFAKRQGTSEDTMRFLYDGGRVHADQTPEDLDMDDGDTIDAFRAQIGGC
H.sapiens SUMO1 : --EYIKLKVIGQDSSEIHFKVKMTTHLKKLKESYCQRQGVPMNSLRFLFEGQRIADNHTPKELGMEEEDVIEVYQEQTGGH
H.sapiens SUMO3 : --DHINLKVAGQDGSVVQFKIKRHTPLSKLMKAYCERQGLSMRQIRFRFDGQPINETDTPAQLEMEDEDTIDVFQQQTGGV
H.sapiens SUMO4 : --NHINLKVAGQDGSVVQFKIKRQTPLSKLMKAYCEPRGLSVKQIRFRFGGQPISGTDKPAQLEMEDEDTIDVFQQPTGGV
A.thaliana SUMO2 : --AHINLKVKGQDGNEVFFRIKRSTQLKKLMNAYCDRQSVDFNSIAFLFDGRRLRAEQTPDELEMEDGDEIDAMLHQTGGG
A.thaliana SUMO3 : --AHVILKVKSQDGDEVLFRNKKSAPLKKLMYVYCDRRGLKIDAFAFIFNGARIGGLETPDELDMEDGDVIDAQRAMSGGL
A.thaliana SUMO1 : --AHINLKVKGQDGNEVFFRIKRSTQLKKLMNAYCDRQSVDMNSIAFLFDGRRLRAEQTPDELDMEDGDEIDAMLHQTGG-
KV F K L F G P L M D GG

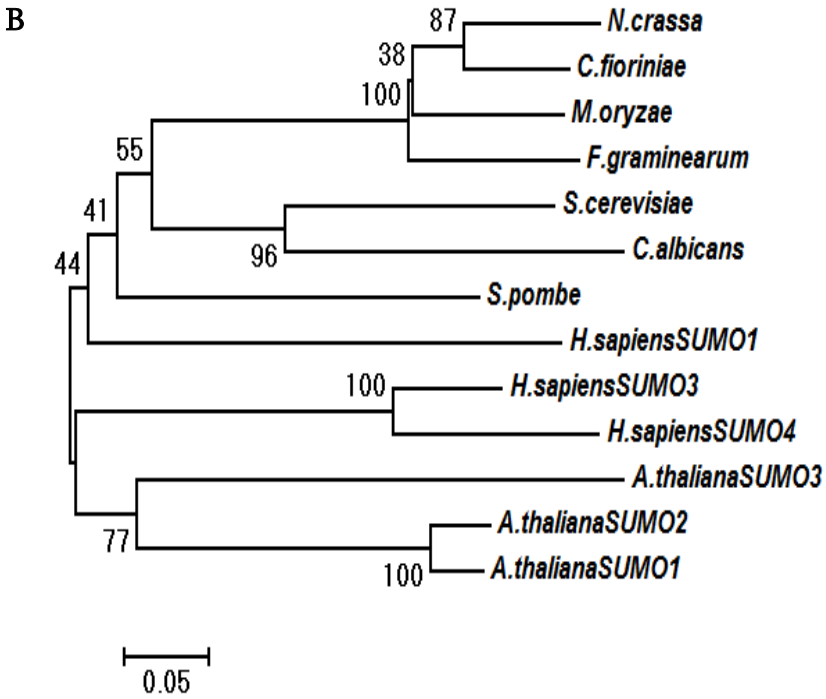
B
87
38
100
55
41
96
44
100
77
100
N.crassa
C.fioriniae
M.oryzae
F.graminearum
S.cerevisiae
C.albicans
S.pombe
H.sapiensSUMO1
H.sapiensSUMO3
H.sapiensSUMO4
A.thalianaSUMO3
A.thalianaSUMO2
A.thalianaSUMO1
0.05

4.2 Complementation of *smt3 (SUMO)* mutant of *S. cerevisiae* with *MoSUMO*

Complementation of *MoSUMO* gene was carried out in *smt3* mutant of *S. cerevisiae* (SBY331). *MoSUMO* gene was cloned in yeast expression vector pYES2.0 and transformed in SBY331 strain (smt3-331) resulting in *smt3-331*-pYes-MoSUMO strain. This strain has a tandem array of lactose operators (lacO) integrated at the *TRP1* locus, 12 kb from the centromere of chromosome IV. A GFP-lactose repressor fusion (GFP-lacI) was expressed in these cells to allow the visualization of chromosome IV. The *smt3* mutant cells showed large budded cells with short spindles and only one bud cell showed GFP signal confirming chromosome segregation defect when held at the nonpermissive temperature of 37^0C for 4hr. The transformants were selected on uracil drop-out SD media supplemented with required amino acids (Figure 7A). To analyze sister chromatid separation, the wild type (SBY214), *smt3-331* and *smt3-331*-pYes-MoSUMO cells were shifted to non-permissive temperature (37^0C) and visualized by confocal microscopy to check chromosomal segregation (on the basis of GFP signal) in the cells. DAPI staining was also performed simultaneously. Majority of the cells showed separated sister chromatids in *smt3-331*-pYes-MoSUMO transformants as well as in wild type compared to SBY331 strain (Figure 7B) indicating that chromosome segregation defect is restored by MoSUMO. These results confirmed that MoSUMO complements the function of SMT3 in *S. cerevisiae* as the defective phenotype was restored in complemented transformants.

4.3 Site directed mutagenesis of MoSUMO diglycine motif and its expression in *S. cerevisiae*

The existence of the diglycine motif in MoSUMO protein is the hallmark of the SUMO conjugation process as it is the key motif for sumoylation pathway. To verify the role of diglycine motif of MoSUMO, C-terminal diglycine (GG) of MoSUMO protein was replaced with dialanine (AA) by site directed mutagenesis (Figure 8A) and transformed into SBY331 strain (*smt3* mutant) resulting MoSUMOgg strain. The transformants were selected on SD media supplemented with the required amino acids. The transformants exhibited a phenotype similar to *smt3* mutant having defective nuclear segregation and accumulation of large budded cells with abnormal GFP signal. The DAPI staining and GFP signals confirmed that sister chromatids were not segregated properly in MoSUMO*gg* transformant (Figure 8B). This result confirmed that diglycine motif of MoSUMO is indispensable for MoSUMO in the conjugation process.

Figure 7: Functional complementation of *MoSUMO* in *S. cerevisiae*

A. Selection of yeast transformants on SD media without uracil at 30°C. 1,2,3,4,5-pYes-MoSUMO transformants, SBY331- *smt3* (*sumo)* mutant strain.

B. Analysis of nuclear segregation in wild type, *smt3* mutant, MoSUMO complemented strain in *S. cerevisiae.* SBY214, SBY331, SBY331-MoSUMO and SBY331-MoSUMO*gg* strains shifted to 37°C for 4hr and analyzed with confocal laser microscopy. Nuclei were stained by DAPI simultaneously indicated by arrowheads. Bar-10μm.

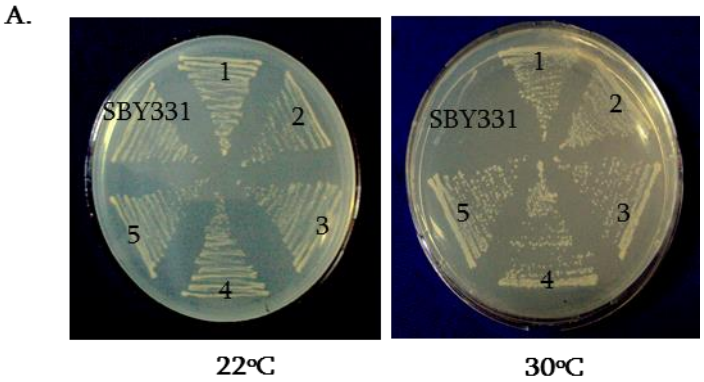
A.
SBY331
1
2
3
4
5
22ºC
SBY331
1
2
3
4
5
30ºC

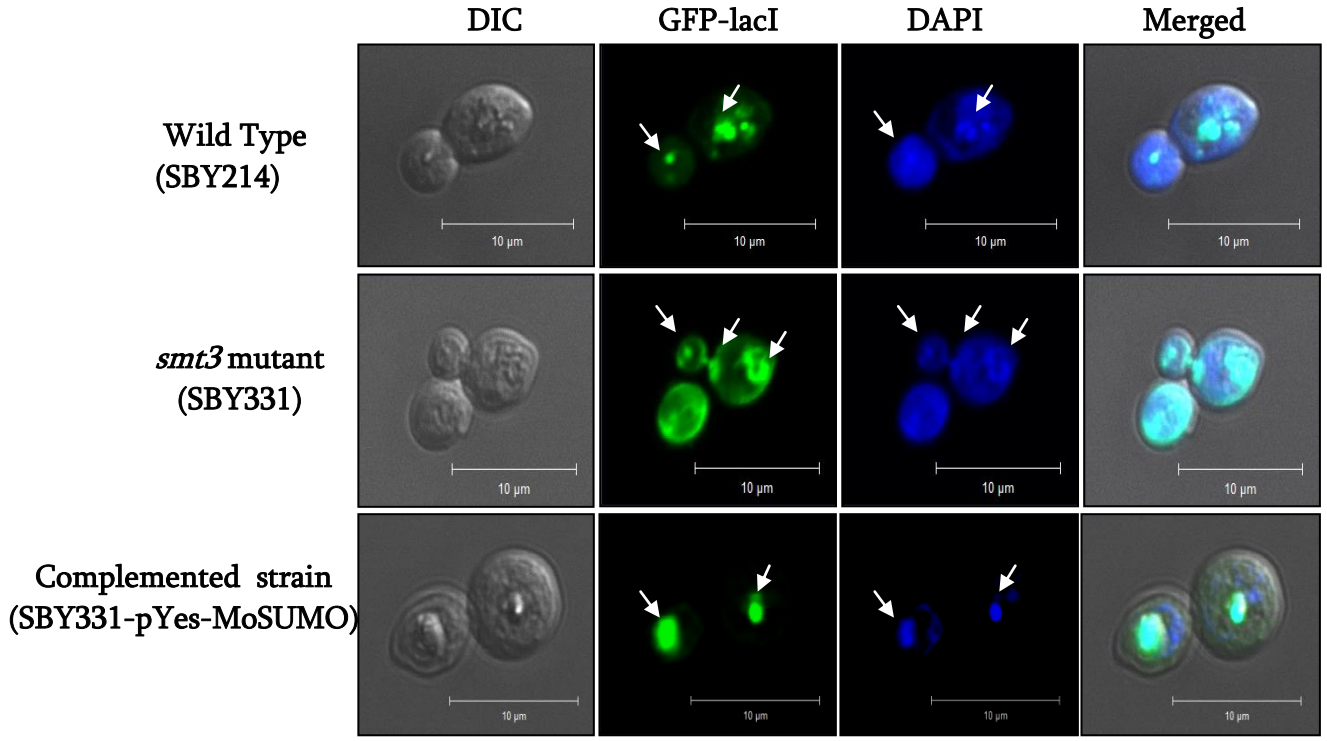
DIC
GFP-lacI
DAPI
Merged
Wild Type
(SBY214)
smt3 mutant
(SBY331)
Complemented strain
(SBY331-pYes-MoSUMO)
10 µm

Figure 8: Phenotype of site directed mutagenized transformant of *S. cerevisiae*

A. Scheme to illustrate the site directed mutation of diglycine motif of MoSUMO with dialanine.

B. Analysis of nuclear segregation in wild type and diglycine mutated strain SBY331 (pYes-*MoSUMOgg*). Nuclear staining (DAPI) was done simultaneously indicated by arrowheads. Bar-10µm.

A.

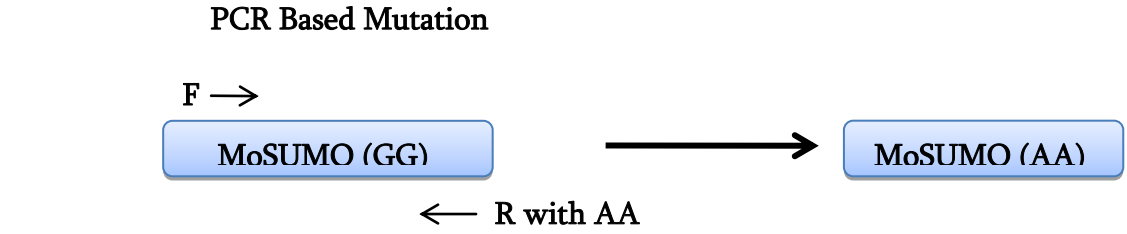
PCR Based Mutation
F
MoSUMO (GG)
MoSUMO (AA)
R with AA

B.

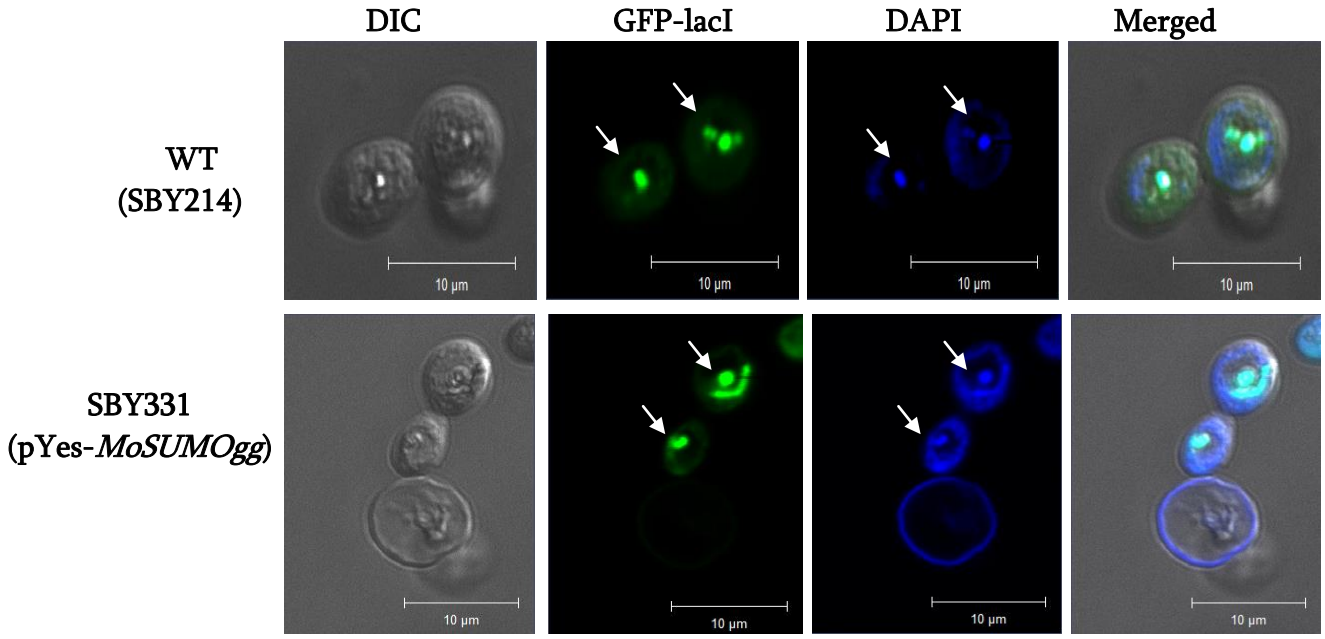
DIC
GFP-lacI
DAPI
Merged
WT
(SBY214)
SBY331
(pYes-*MoSUMOgg*)
10 µm

4.4 Molecular characterization of *ΔMosumo* mutant and complemented strain

A knock-out construct was generated using the split marker approach to characterize the functional role of *MoSUMO* in *M. oryzae* (Figure 4). The wild type B157 was transformed with split markers of *MoSUMO* using protoplast transformation. The resulting hygromycin resistant transformants were screened by PCR using *MoSUMO* gene specific primers and β tubulin gene amplification was used as a positive control. No amplification of *MoSUMO* gene was observed in KO1, KO3 and KO4 transformants (Figure 10B). These transformants were further analyzed by Southern hybridization. Knock-out transformants were confirmed using three different probes (Figure 10A). When the blot of *Nco*I digested genomic DNA of wild type and transformants was hybridized with 'probe a' (5'flanking region), two bands of 3.3 kb and 1.1 kb were observed in the wild type while as in transformants, 1.8 kb and 1.1 kb bands were observed (Figure 10C). When the same blot was hybridized with 'probe b' (3'flanking region) after stripping, a 3.3 kb band and a 2.9 kb band were obtained in the wild type and in transformants, respectively (Figure 10C). These transformants were further confirmed with 'probe c' (*MoSUMO* gene) using the same blot after stripping. A single band was obtained in the wild type while no band was observed in transformants (Figure 11C). Analysis of all the three blots showed the expected band pattern and confirmed that KO1, KO3 and KO4 were three independent *ΔMosumo* null mutants. Expression analysis using RT-PCR further confirmed the absence of

MoSUMO transcript (Figure 11). β-tubulin gene was used as a positive control and rRNA was used as the control for equivalent concentration of corresponding gene amplification. Phenotypes of all the three mutants were identical in terms of growth, conidiation and pathogenicity, therefore, KO1 (hereafter referred as *ΔMosumo*) was used in subsequent experiments.

Complementation was carried out by reintroducing a *MoSUMO* allele in *ΔMosumo* mutant strain to ensure the phenotype exhibited by *ΔMosumo* null mutant was due to the deletion of *MoSUMO* gene (Figure 5). A 3.7 kb complementation construct carrying *MoSUMO* gene with zeocin selection marker was generated. The *ΔMosumo* mutant was transformed using this construct by protoplast mediated fungal transformation. The transformants were screened on YEG plates containing zeocin and hygromycin separately (Figure 12A), and transformants which were resistant to zeocin and sensitive to hygromycin were selected for further analysis and confirmed by Southern blot analysis. The genomic DNA of wild type and transformant digested with *EcoR*I and hybridized with 'probe a' (comprising of TAP-*MoSUMO* and zeocin gene) (Figure 12B) gave two bands in the transformant and a single band in the wild type (Figure 12C- Left Panel). These transformants were further confirmed using different restriction enzymes like *Nco*I, *Nde*I, *BamH*I and *Xba*I, hybridized with 'probe b' (comprised of promoter region and TAP-*MoSUMO* gene) (Figure12B) and expected band

pattern was obtained (Figure 12B-Right panel). The hybridization pattern showed that hygromycin was replaced with zeocin cassette. This transformant was further referred as *ΔMosumo*/*MoSUMO* (complemented) strain.

4.5 Phenotypic characterization of *ΔMosumo* mutant and *ΔMosumo*/*MoSUMO* complemented strain

The phenotypic characterization of *ΔMosumo* mutant and complemented strain was carried out by examining growth pattern, conidiation, appressorial development and pathogenicity of the fungus.

4.5.1 Growth

The *MoSUMO* was not essential for viability in *M. oryzae* as *MoSUMO* deletion mutant was viable. Wild type, *ΔMosumo* mutant and *ΔMosumo*/*MoSUMO* complemented transformants were allowed to grow for 5 days. The aerial hyphae and melanin content were observed and no detectable difference was found in these strains (Figure 13A and B). The growth of *ΔMosumo* mutant was dramatically reduced compared to wild type whereas the complemented strain rescued this defect (Figure 13B and C).

4.5.2 Conidiation

Conidiation was compared among the wild type, *ΔMosumo* mutant, and *ΔMosum*o/*MoSUMO* strain after growth on OMA for 8 days. The conidia were counted in Neubauer chamber and statistical analysis of conidiation showed

significant reduction in conidiation in *ΔMosumo* mutant compared to wild type. The complemented *ΔMosumo*/*MoSUMO* strain showed comparable conidiation with respect to wild type (Figure 14A). Comparisons of groups were performed using student t-test for repeated measurements to determine the levels of significance for each group. $P<0.05$ was considered as statistically significant.

4.5.3 Appressorium development

The conidia of wild type, *ΔMosumo* mutant and *ΔMosumo*/*MoSUMO* strains were assayed on artificial hydrophobic surface for the formation of appressoria. The *ΔMosumo* mutant failed to form appressoria even after 20hr of inoculation on hydrophobic surface whereas complemented strain developed appressoria similar to that of wild type (Figure 13B). Appressorial development was also checked from hyphae of *sumo* mutant. The mycelia of wild type, *ΔMosumo* mutant and complemented strains were placed on hydrophobic surface under high humidity for 48 h and formation of appressoria was observed under microscope. The *ΔMosumo* mutant was not able to form appressoria like wild type and complemented strains (Figure 14C). The number of germinated conidia was statistically analyzed using one way ANOVA and $P<0.05$ value was considered as statistically significant (Figure 14D).

4.5.4 Infection assay

The role of *MoSUMO* in infection was investigated using susceptible rice cultivar CO39. The rice plants were sprayed with 10^5 spores harvested from wide type,

ΔMosumo mutant and complemented strains. The wild type and complemented strains showed typical blast lesions, whereas *ΔMosumo* mutant was unable to elicit any disease symptoms even after 10-15 days (Figure 14D).

4.5.5 Penetration assay using rice leaf sheath

The penetration assay was performed on rice leaf sheath. The conidia of wild type, *ΔMosumo* mutant and *ΔMosumo*/*MoSUMO* strains were inoculated on the leaf sheath and allowed to grow for 36hr. Infected leaf sheath was stained with aniline blue to visualize the fungal mycelia. Microscopic observation showed that the *sumo* deletion mutant was unable to penetrate whereas wild type and *ΔMosum*o/*MoSUMO* strains form hyphal network (Figure 14E).

4.6 Depletion of *MoSUMO* causes defective nuclear segregation and septation

The investigation of cell division in vegetative hyphae demonstrates that sumoylation has an important role in mitosis. Nuclear and cell wall staining exhibited normal distribution of the nucleus in wild type whereas *ΔMosumo* mutant showed two nuclei in a single cell (Figure 15). Most of the mycelial cells had abnormal distribution of nuclei, indicating nuclear segregation defect. In addition to this defect, an increased number of septa was also observed during germination of conidia in *ΔMosumo* mutant compared as to the wild type.

Figure 9: Cloning strategy for split marker and clone confirmation.

Hygromycin phosphotransferase (HPT) gene, 5'flanking (5'F) and 3'flanking (3'F) region were amplified and cloned in pBluescript KS+ at *Eco*RV site, schematically represented in A, B and C Respectively. The confirmation of KS-HPT, KS-5'F and KS-3'F clones using different restriction enzymes.

A. KS-HPT (Lane 1-HindIII, Lane 2- *PstI,* Lane 3-*Eco*RI, Lane 4- DNA Marker)

B. KS-5'F (Lane1- DNA Marker, Lane 2- *Pst* I)

C. KS-3'F (Lane 1-*Sal* I, Lane 2- DNA Marker)

D. KS-5'F clone was digested with *Bam*HI and cloned in KS-HPT clone at same site to obtain KS-5'F-HPT clone. Lane 1- *Xho* I, Lane 2- *Nco* I, Lane 3- DNA Marker.

E. KS-3'F clone was digested with *Xho*I and cloned in KS-HPT clone at same site to obtain KS-3'F-HPT clone. Lane 1- DNA Marker, Lane 2- *Sal* I, Lane 3-*Xho* I.

F. Split markers used for protoplast transformation. Lane 1- 5'F-HP amplified product, Lane 2- PT-3'F amplified product, Lane 3-DNA Marker.

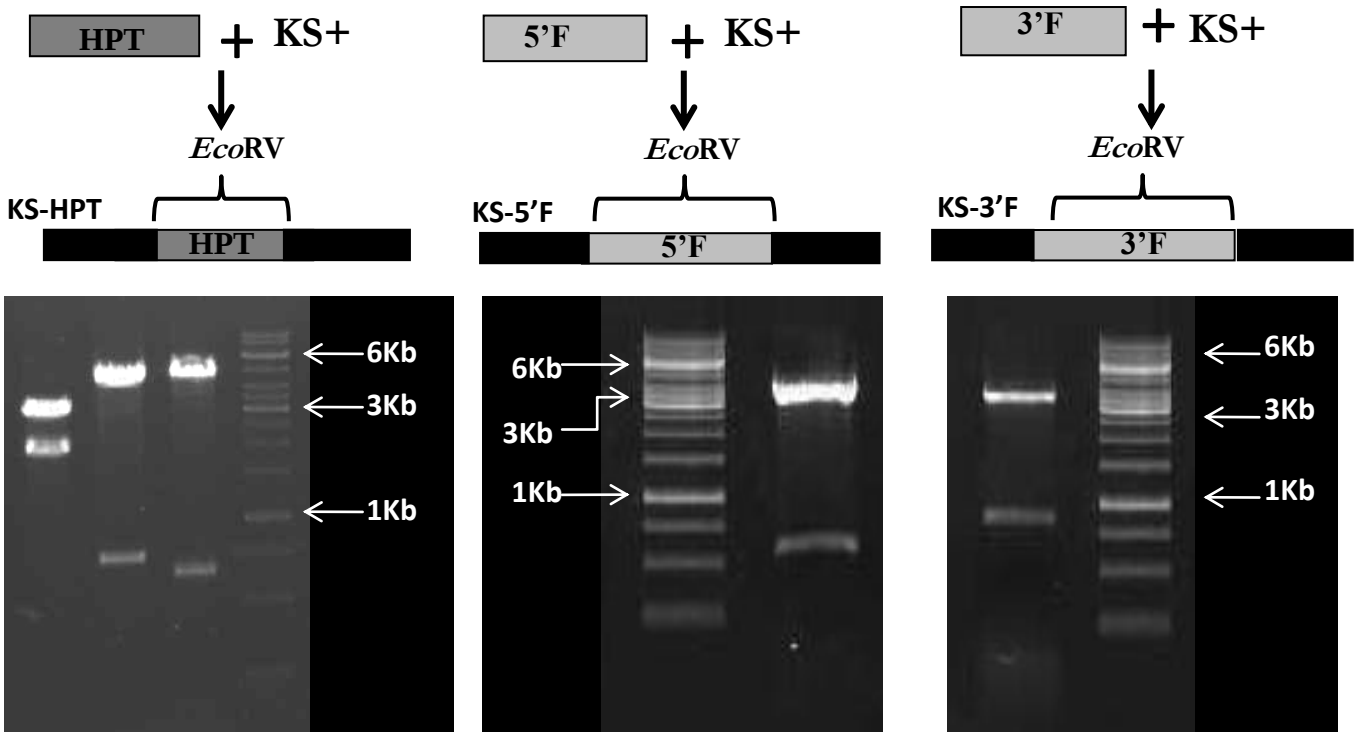
HPT
+ KS+
EcoRV
KS-HPT
HPT
6Kb
3Kb
1Kb
5'F
+ KS+
EcoRV
KS-5'F
5'F
6Kb
3Kb
1Kb
3'F
+ KS+
EcoRV
KS-3'F
3'F
6Kb
3Kb
1Kb

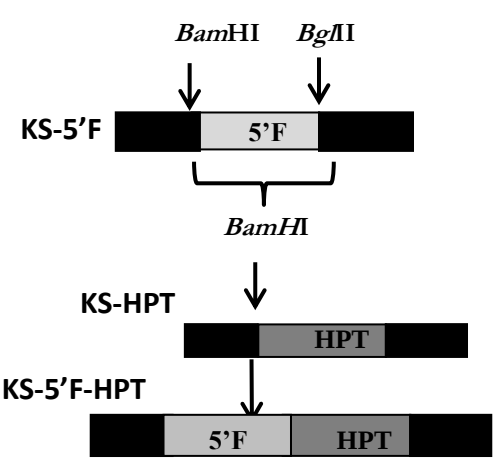

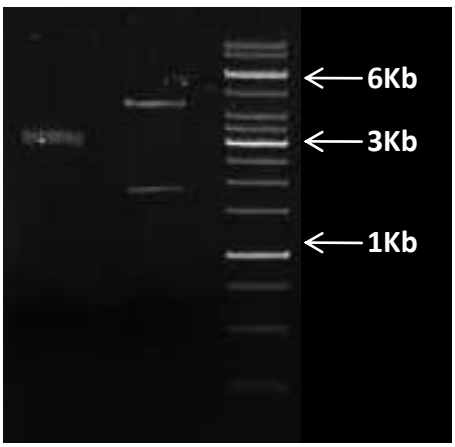

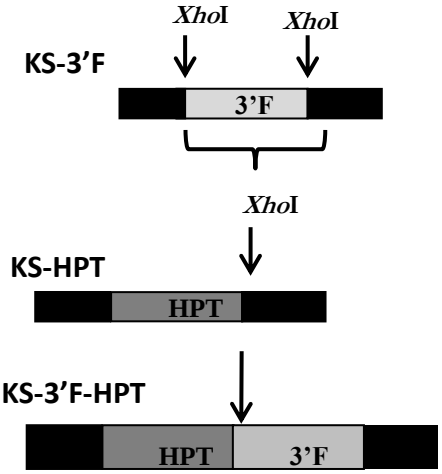

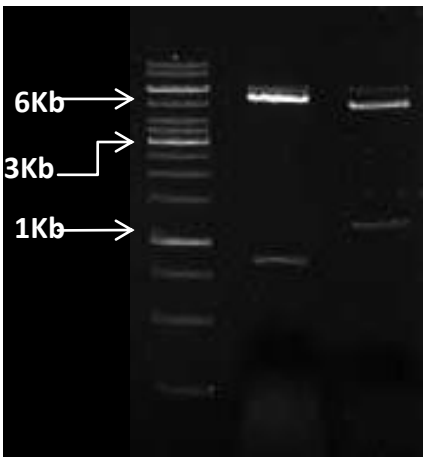

Split markers used for protoplast transformation

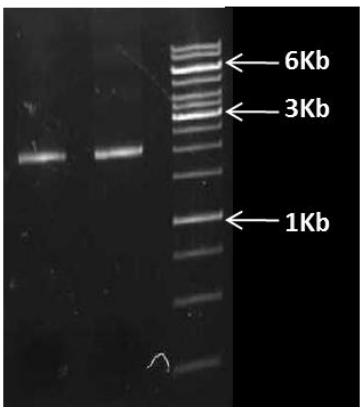

Figure 10: Targeted deletion of *MoSUMO* gene in *M. oryzae* using split marker approach.

A. Schematic representation of knock-out construct of *MoSUMO*. *MoSUMO* is flanked by homologous gene sequences (5'F and 3'F) allowing homologous recombination between genomic DNA.

B. Screening of putative knock-out transformants by PCR using *MoSUMO* gene specific primers (Upper panel) and tubulin gene amplification for positive control (Lower panel).

C. Southern blot analysis of knock-out mutants using three probes; genomic DNA of wild type (WT) and knock-out transformants (KO1, KO2, KO3 and KO4) digested with *Nco*I (N) and hybridized with a.probe, b. probe and c. probe.

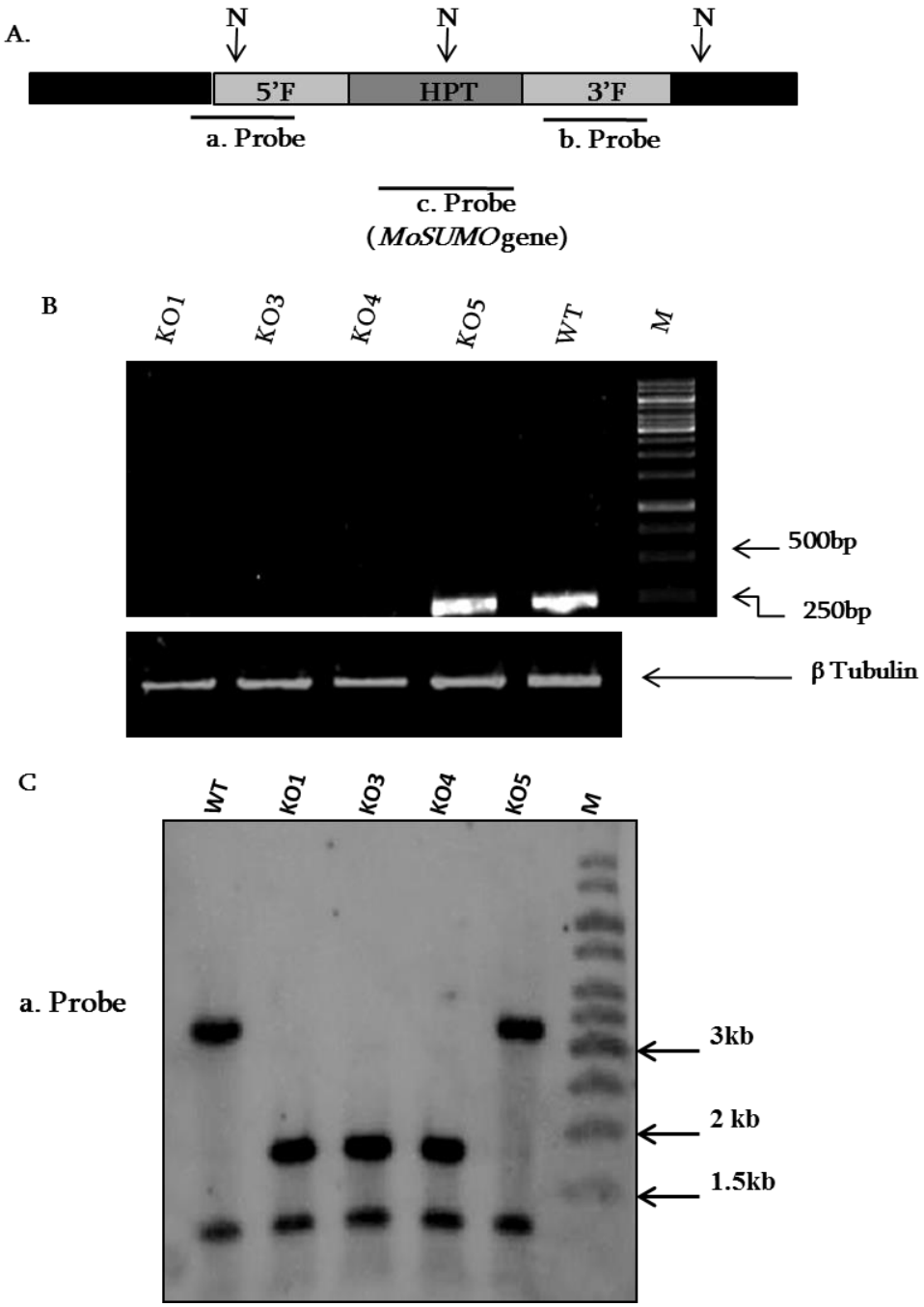
A.
N
N
N
5'F
HPT
3'F
a. Probe
b. Probe
c. Probe
(MoSUMOgene)
B
KO1
KO3
KO4
KO5
WT
M
500bp
250bp
β Tubulin
C
WT
KO1
KO3
KO4
KO5
M
a. Probe
3kb
2 kb
1.5kb

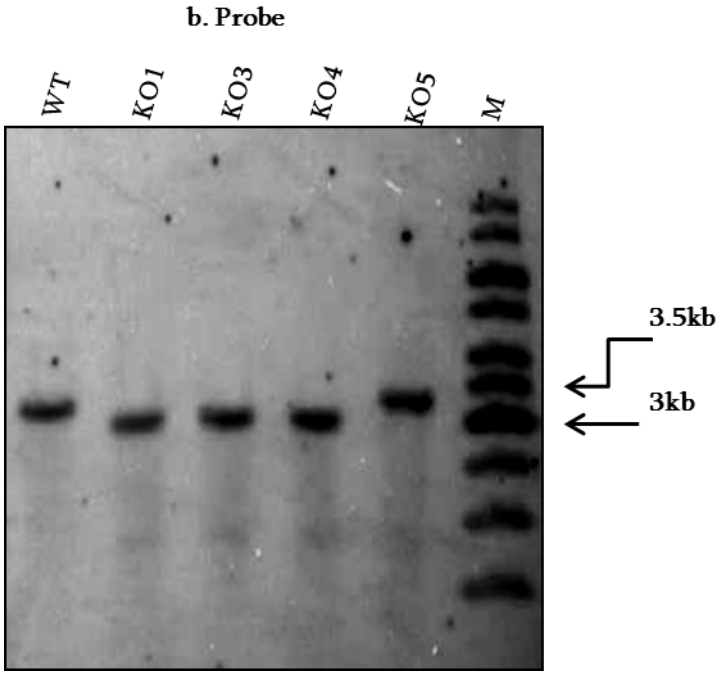
b. Probe
WT
KO1
KO3
KO4
KO5
M
3.5kb
3kb

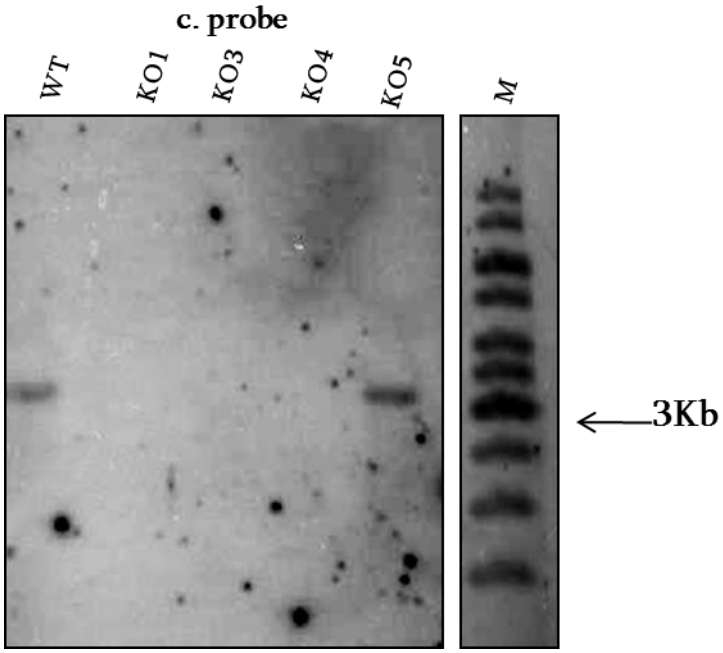
c. probe
WT
KO1
KO3
KO4
KO5
M
3Kb

Figure 11: Reverse Transcriptase-PCR of wild type and *ΔMosumo* mutant

The absence of *MoSUMO* transcripts was checked in *ΔMosumo* mutant using RT-PCR and *β*-Tubulin taken as internal control. Upper panel: Lane1-5- *MoSUMO* from cDNA, Lane 2-5-KO1, KO3, KO4 and KO5 transformants, Lane 6- *MoSUMO* from genomic DNA and Lane7-Marker. Middle panel-*β*-Tubulin gene amplification from corresponding cDNA and genomic DNA. Lower panel: rRNA from corresponding RNA samples indicating equivalent loading of RNA.

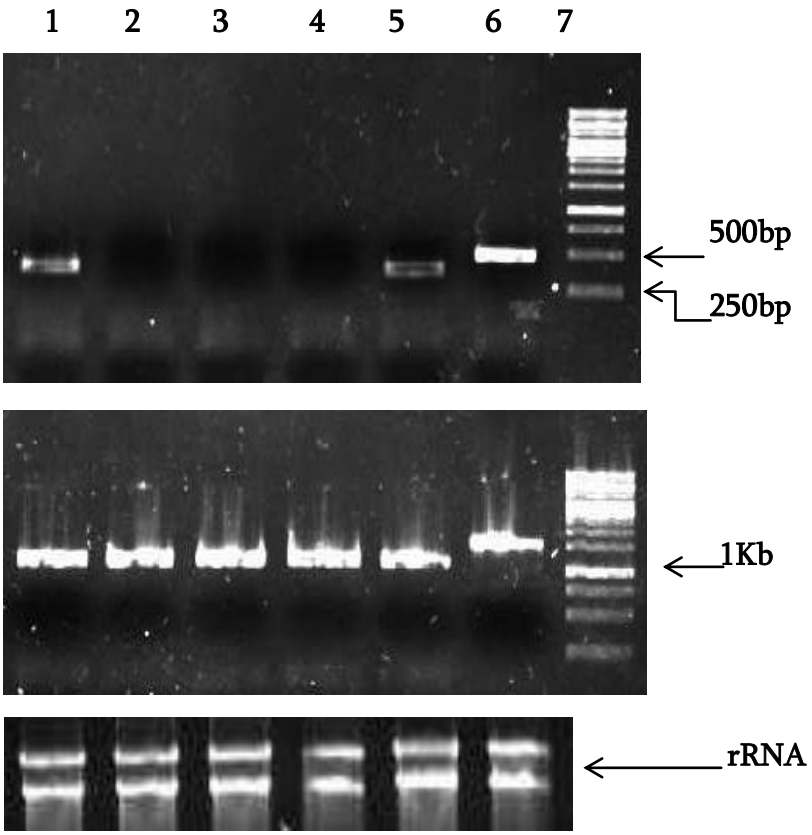
1
2
3
4
5
6
7
500bp
250bp
1Kb
rRNA

Figure 12: Complementation *MoSUMO* gene in *M. oryzae*

A. Complemented transformants (*ΔMosumo*/*MoSUMO*) were selected on YEG plates containing zeocin and hygromycin separately.

B. Schematic representation of complementation strategy to illustrate the replacement of a HPT gene in *ΔMosumo* mutant strain with *MoSUMO* under native promoter and zeocin for selectable marker, flanked by homologous gene sequence facilitates homologous recombination between genomic DNA. Probes were designated by a and b.

C. Southern blot analysis of complemented transformant using probe a and b. Genomic DNA of wild type (WT) and putative knock-out transformant digested with *EcoR*I (E) and hybridized with probe a. resulted in two bands in transformant and single band in WT (Left Panel). This transformant further digested with different restriction enzymes like *Nco*I(N), *Nde*I(Nd), *BamH*I(B) and *Xba*I(X), hybridized with probe b. and showed the expected band pattern, confirming the replacement cassette and further referred as *ΔMosumo*/*MoSUMO* transformant (Right panel).

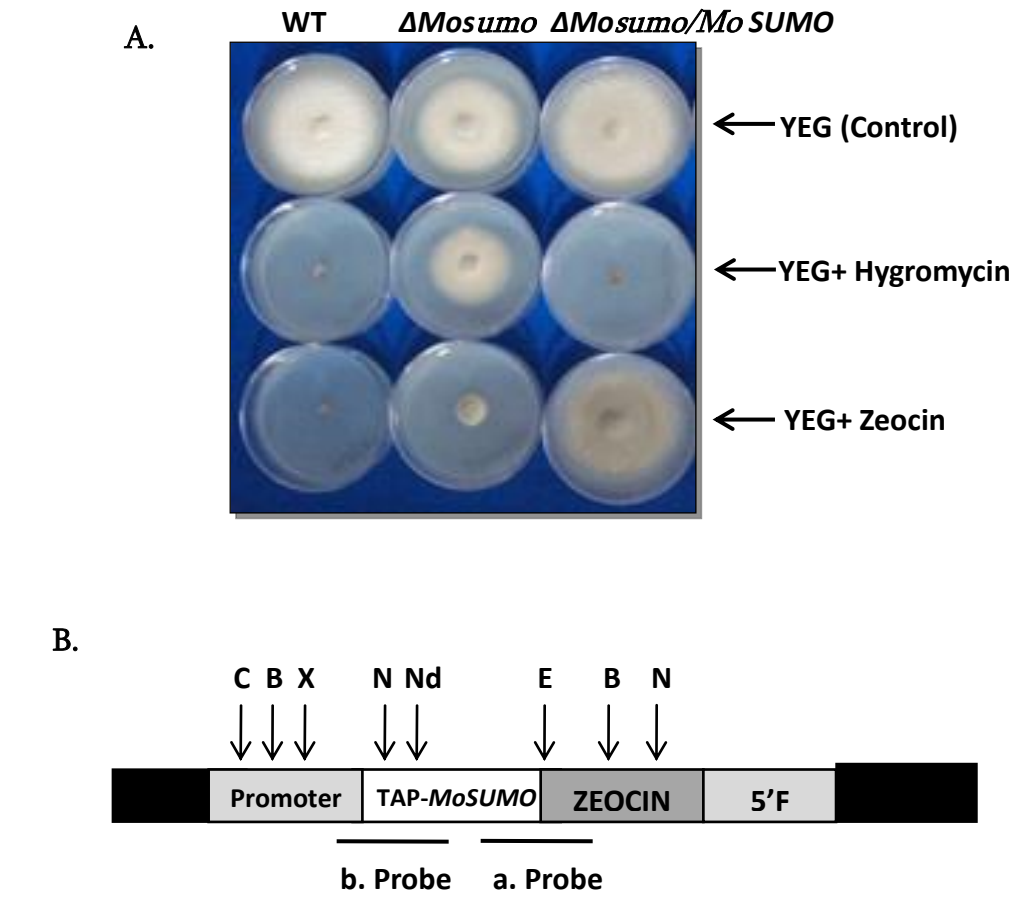
A.
WT
ΔMosumo
ΔMosumo/Mo SUMO
YEG (Control)
YEG+ Hygromycin
YEG+ Zeocin
B.
C B X
N Nd
E
B
N
Promoter
TAP-MoSUMO
ZEOCIN
5'F
b. Probe
a. Probe
C.
Probe a
Probe b
WT
ΔMosumo/Mo SUMO
N
Nd
B
X
M
5 kb
2.5 kb
6Kb
3Kb

Figure 13: Growth assay of *ΔMosumo* mutant and complemented strain (*ΔMosumo/MoSUMO)*

A. Growth of wild type (WT) and *ΔMosumo* strains on YEG medium showing similar aerial hyphae (upper panel) and melanin content (lower panel), after 2-5 days of incubation at 28^0C.

B. Five day old culture of wild type, *ΔMosumo* mutant and complemented strain (*ΔMosum*o/*MoSUMO*) on OMA.

C. Growth pattern of wild type, *ΔMosumo* mutant and *ΔMosum*o/*MoSUMO* strain at successive days of incubation on OMA.

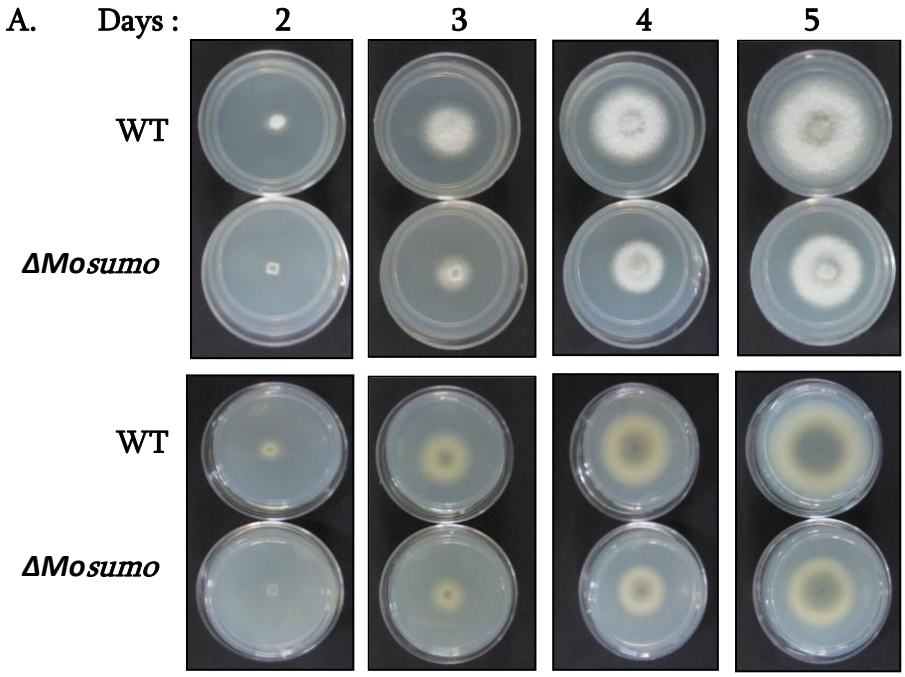
A.
Days :
2
3
4
5
WT
ΔMosumo
WT
ΔMosumo

B.

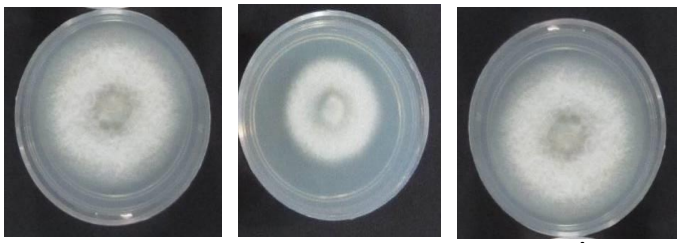
WT
ΔMosumo
ΔMosumo/MoSUMO

C.

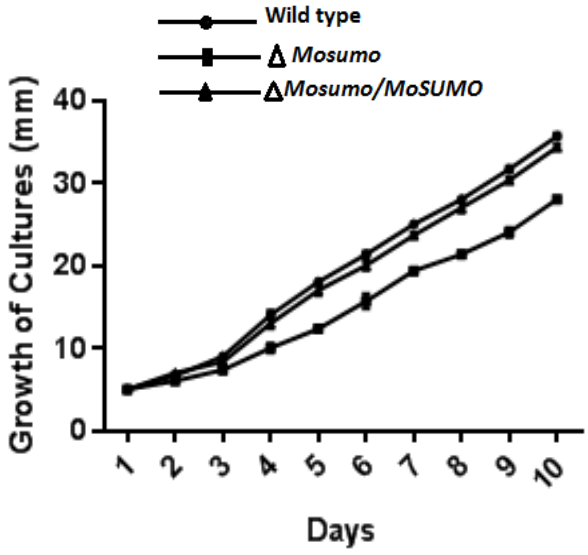
Wild type
ΔMosumo
ΔMosumo/MoSUMO
Growth of Cultures (mm)
0
10
20
30
40
1
2
3
4
5
6
7
8
9
10
Days

Figure 14: Phenotype of wild type, *ΔMosumo* mutant and complemented strains

A. Conidiation was compared among wild type, *ΔMosumo* mutant, and *ΔMosumo*/*MoSUMO* strains after growth on OMA for 8 d. Mean and Standard error (SE) were calculated from three independent replicates. Asterisks indicate significant differences. T-test $P<0.05$.

B. Development of appressorial was affected in wild type, *ΔMosumo* mutant, and *ΔMosumo*/*MoSUMO* strains. Strains were grown on OMA for 7 days were examined by light microscopy. *ΔMosumo* mutant was unable to develop appressorium like WT and *ΔMosumo*/*MoSUMO* strains.

C. The number of conidia germination was checked on hydrophobic slide and analyzed statistically using one way ANOVA. $P<0.05$.

D. Hyphal blocks of the wild type, *ΔMosumo* mutant and *ΔMosumo*/*MoSUMO* strains were placed on hydrophobic coverslips, placed in dark at 28^0C under high humidity and imaged after 24h.

E. Three week old rice leaves of CO39 were sprayed with spore suspension (~10^5spores/ml) of wild type, *ΔMosumo* mutant and *ΔMosumo*/*MoSUMO* strains. Disease symptoms were assessed after 10 days.

F. Rice leaves were inoculated with conidial suspensions of wild type, *ΔMosumo* mutant and *ΔMosumo*/*MoSUMO* strains. The invasive hyphae were examined after 36 hpi. *MoSUMO* deletion mutants is defective in development of infectious hyphae however Wild type and *ΔMosumo*/*MoSUMO* strains. Bar -10 μm.

A.

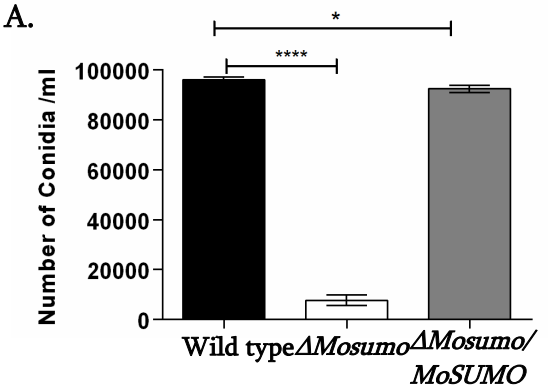
*
****
Number of Conidia /ml
100000
80000
60000
40000
20000
0
Wild type
ΔMosumo
ΔMosumo/ MoSUMO

C.

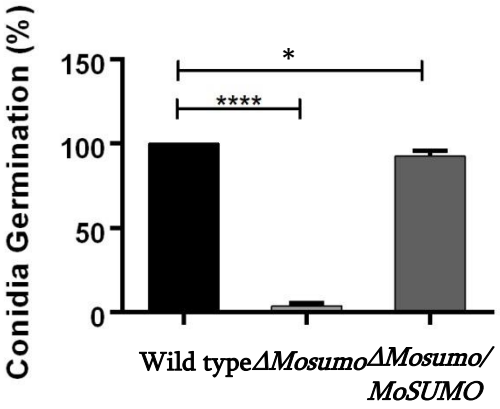
Conidia Germination (%)
150
100
50
0
*
****
Wild type
ΔMosumo
ΔMosumo/ MoSUMO

B.

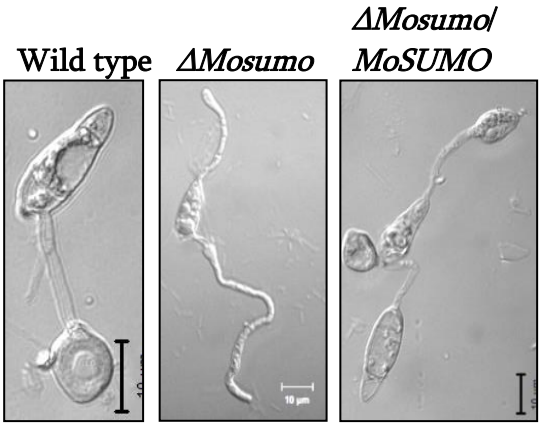
Wild type
ΔMosumo
ΔMosumo/ MoSUMO

D.

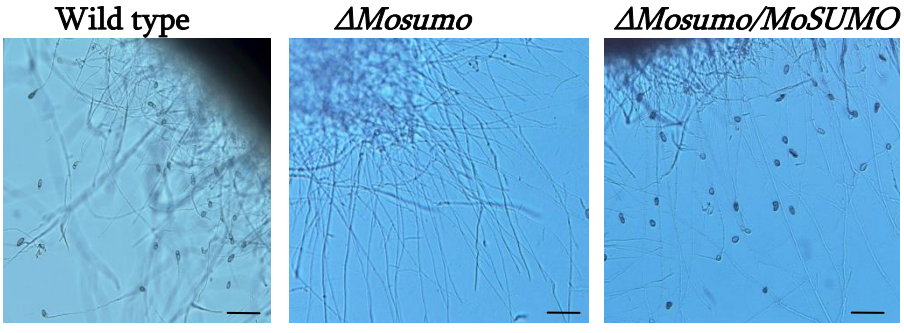
Wild type
ΔMosumo
ΔMosumo/MoSUMO

E.

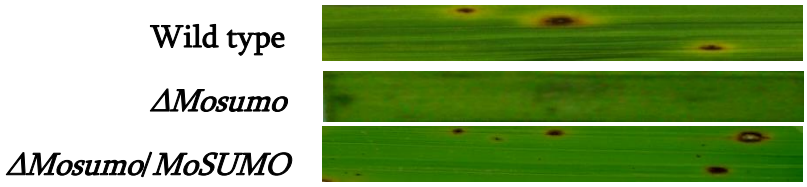
Wild type
ΔMosumo
ΔMosumo/MoSUMO

F.

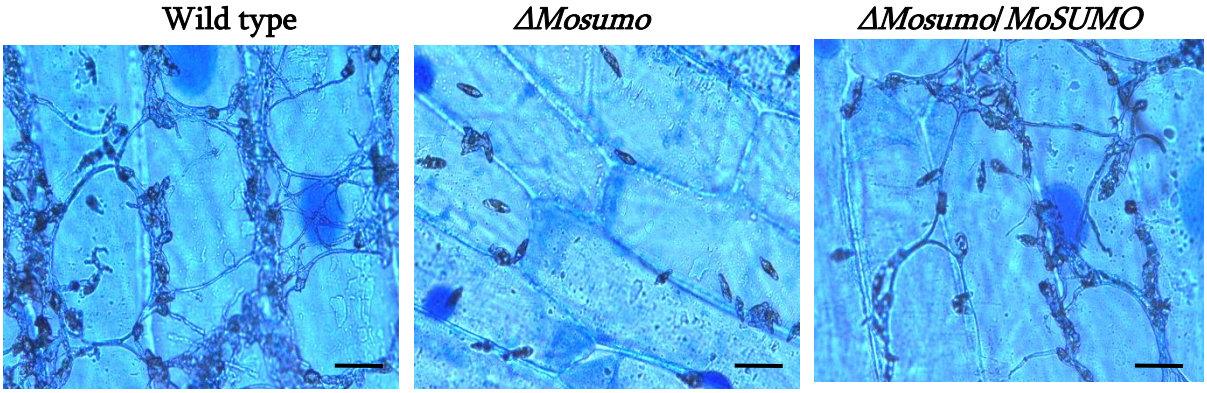
Wild type
ΔMosumo
ΔMosumo/MoSUMO

Figure 15: Nuclear segregation in Wild type and *ΔMosumo* mutant

DAPI and CFW staining of Wild type and *ΔMosumo* mutant in hyphae, showed single nucleus in Wild type cell whereas *ΔMosumo* mutant had multinucleated phenotype indicated by arrowhead. DAPI+CFW-Left panel, DIC- Right panel. Bar-10μm.

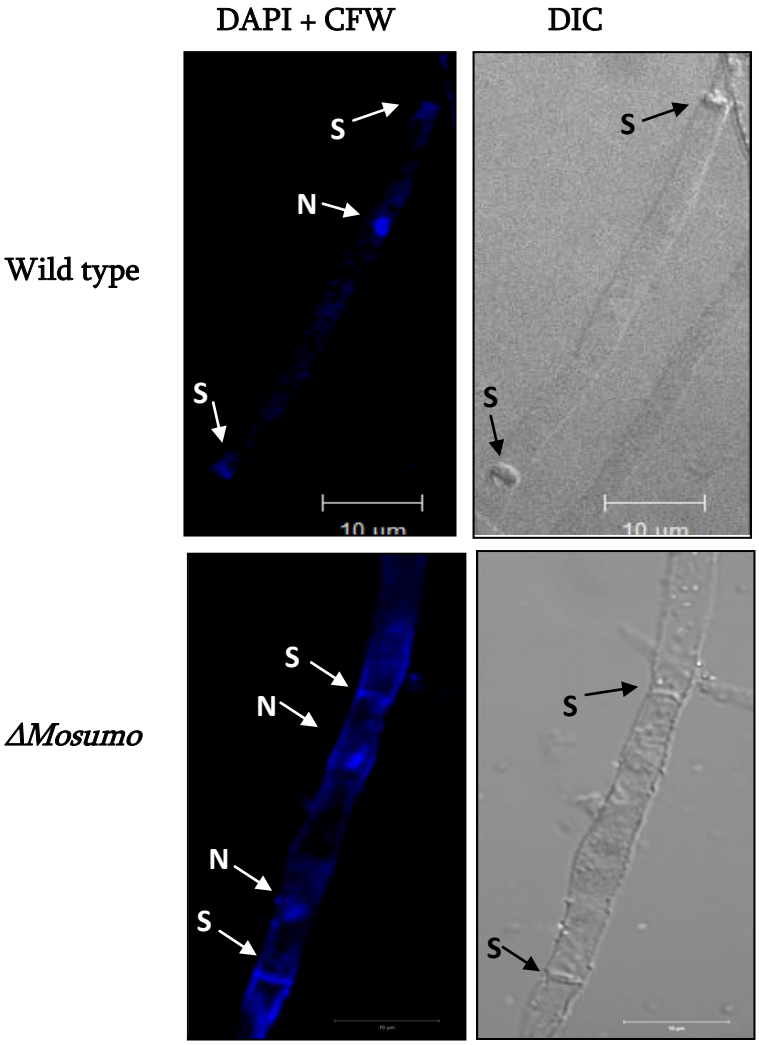
DAPI + CFW
DIC
Wild type
S
N
S
10 µm
S
S
10 µm
ΔMosumo
S
N
N
S
S
S

4.7 *ΔMosumo* mutant exhibits aberrant chitin deposition in developmental stages of conidia

CFW staining was performed to check chitin deposition in hyphae, conidia and appressoria of wild type and *ΔMosumo* mutant. A normal distribution of chitin was observed in both the mycelia of wild type and *ΔMosumo* mutant (Figure 16). However, during development of appressoria from conidia, *ΔMosumo* mutant showed abnormal chitin deposition, irregular shape and septation in the germ tube (Figure 16).

4.8 Heterologous protein expression in *E.coli* and raising an antibody against MoSUMO

The fusion protein GST-MoSUMO was expressed in *E. coli* BL21 (DE3) pLysS strain and was purified using glutathione sepharose 4B resin according to manufacturer's instruction. The fusion protein fraction was checked on 12% SDS-PAGE where it showed a single fragment of 38 KD (26 Kd of GST + 12 Kd of MoSUMO) when stained with Coomassie Blue. The fusion protein was cleaved with factor Xa to release MoSUMO protein (12Kd) (Figure 17B) which was then purified using glutathione sepharose 4B resin. Polyclonal antibody was raised against MoSUMO protein and the titer value for the antibody was found to be 1000.

Figure 16: Chitin distribution in Wild type and *ΔMosumo* mutant

Chitin staining of mature and defective appressoria of Wild type and *ΔMosumo* mutant respectively indicates aberrant chitin deposition and abnormal septation in *ΔMo*sumo mutant shown by arrowheads. Number of septation was more in germinating conidia of *ΔMosumo* mutant. CFW-Left panel, DIC-Right panel. S-Septum, AP-Appressorium. Bar-10µm.

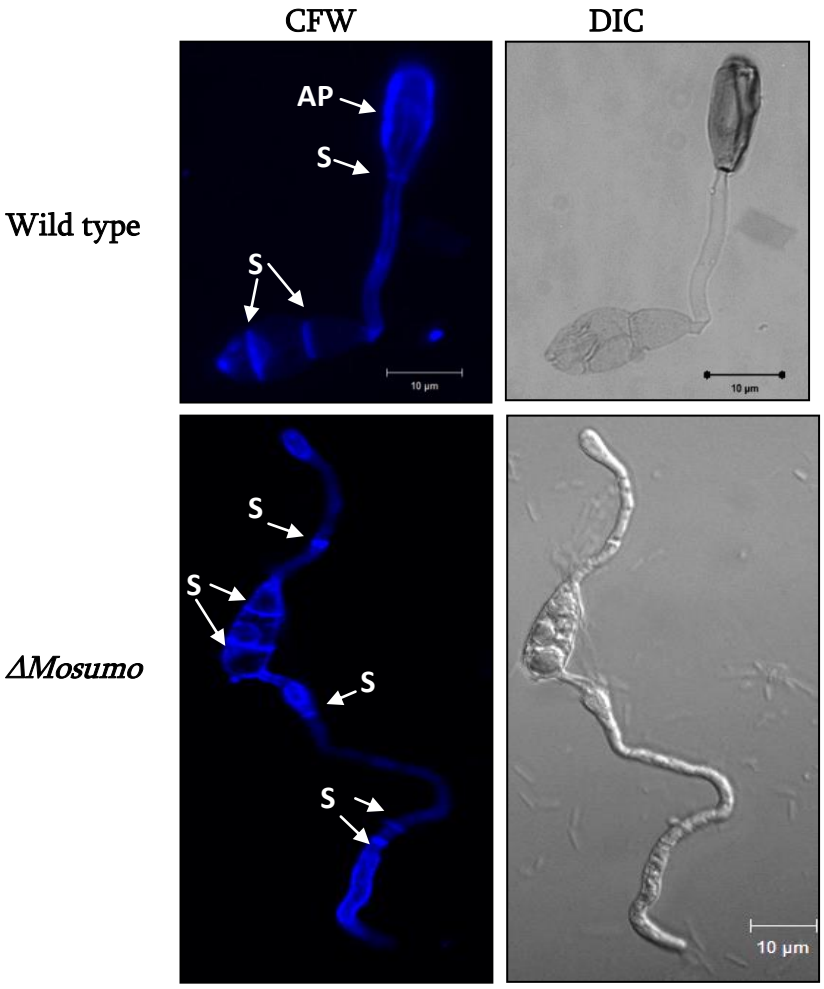
CFW
DIC
Wild type
AP
S
S
10 µm
10 µm
ΔMosumo
S
S
S
S
10 µm

Figure 17: Expression of GST and MoSUMO proteins in *E. coli*

A. Optimization of purification procedure with GST protein and checked on 12% SDS-PAGE. Lane 1 – Total Protein, Lane 2 – Flow through, Lane 3-1st wash, Lane 4- 2nd wash, Lane 5-2nd Elute, Lane 6- 3rd Elute, Lane 7- Protein Marker.

B. Purification of GST-MoSUMO fusion protein and checked on 12% SDS-PAGE followed by CBB staining. Lane 1 – Total Protein, Lane 2 – Flow through, Lane 3-1st wash, Lane 4-1st Elute, Lane 5-2nd Elute, Lane 6- 3rd Elute, Lane 7- Protein Marker.

C. Site specific cleavage of GST-MoSUMO fusion protein with factor Xa. Cleavage of fusion protein was checked on 15% SDS-PAGE and silver staining was carried out. Lane 1-Protein Marker, Lane 2- GST (26Kd) + MoSUMO(12Kd).

D. Purification of MoSUMO from cleaved fusion protein with glutathione sepharose resin and examined on 15% SDS-PAGE followed by silver staining. Lane 1-3-GST protein (26Kd), Lane 2- MoSUMO protein (12Kd).

A.

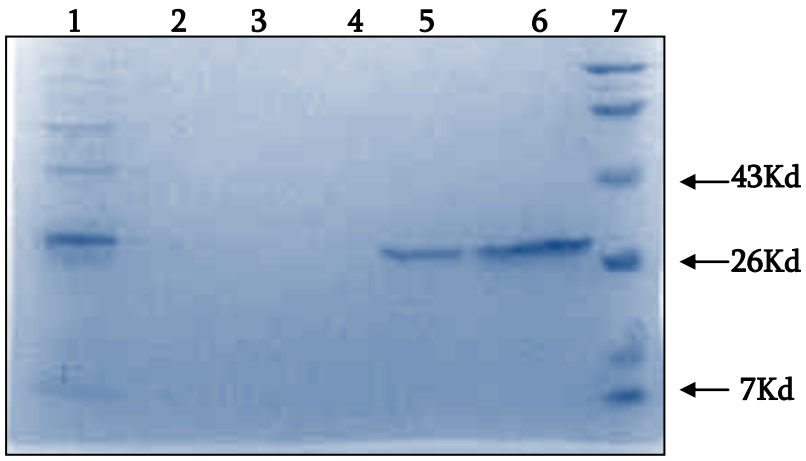

B.

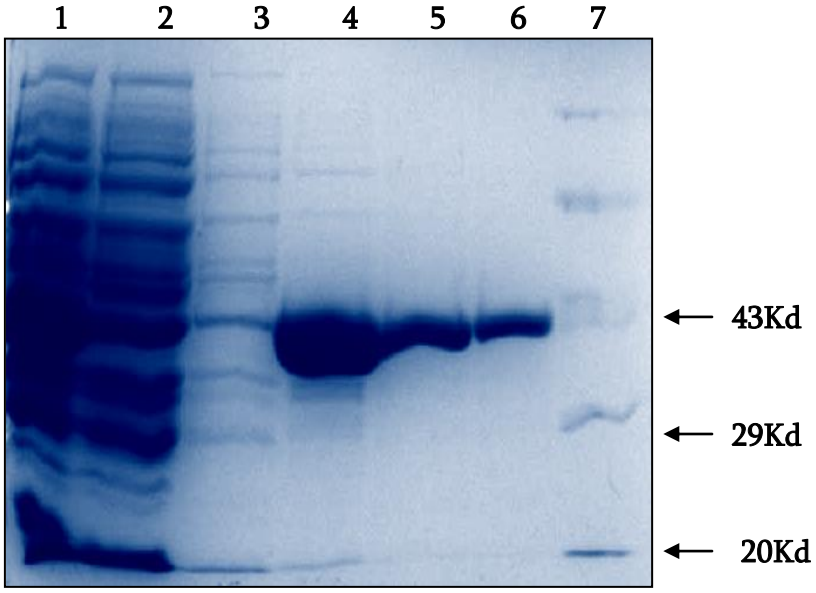

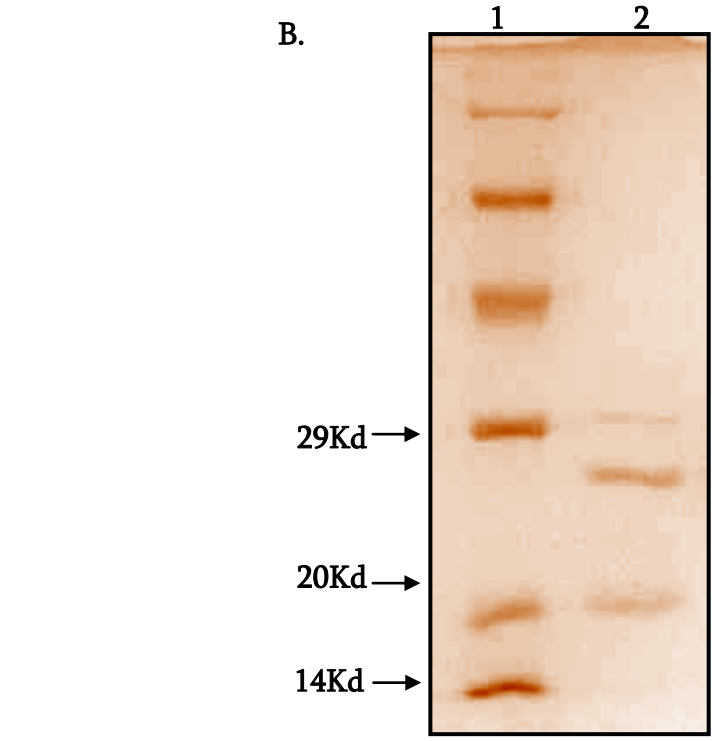
B.
1
2
29Kd
20Kd
14Kd

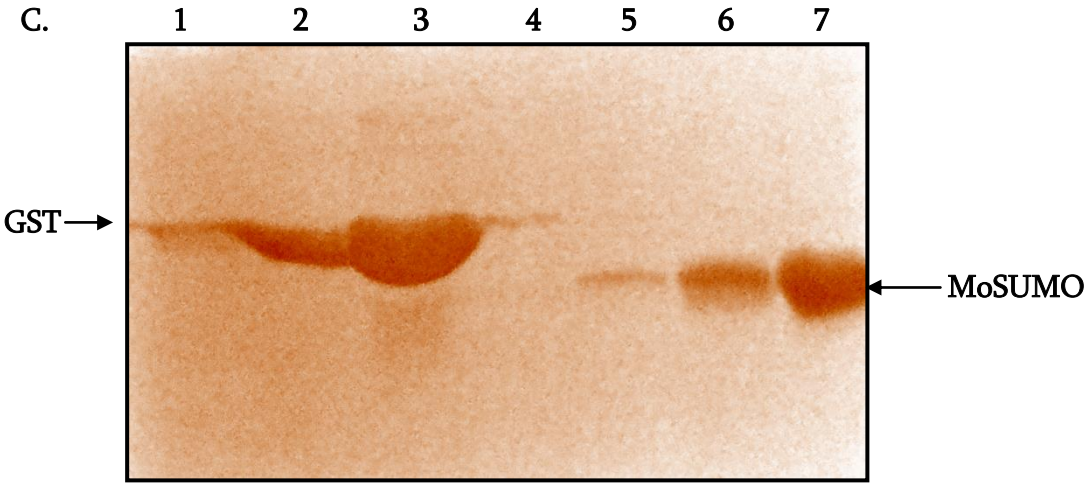
C.
1
2
3
4
5
6
7
GST
MoSUMO

4.9 Immunoblot analysis

Total intracellular proteins were extracted from the mycelia of wild type grown in CM and separated on 12% SDS-PAGE. Anti-SUMO antibody was used to detect SUMO and/or sumoylated proteins. A wide range of protein bands were observed in the immunoblot indicating that multiple proteins were sumoylated (Figure 18). Purified MoSUMO (12Kd) and GST-MoSUMO (38Kd) protein were used as the positive control.

4.10 Subcellular localization of MoSUMO by indirect immunolocalization

TRITC-conjugated secondary antibody was used for immunolocalization. In the hyphae of wild type, fluorescence signal was seen at the septal region (Figure 19A). However, it was observed in septa as well as nuclei of conidia (Figure 19B). These results showed that MoSUMO and/or sumoylated proteins were prominently present in septal and nuclear region of *M. oryzae.*

4.11 Characterization of MoSUMO localization transformant

Subcellular localization of MoSUMO protein was investigated in *M. oryzae*, GFP tag was fused at N-terminus of MoSUMO gene under the control of endogenous MoSUMO promoter with zeocin as selection marker (Figure 20A). A 4.1 kb linear fragment of localization construct was transformed into wild type by protoplast

Figure 18: Western blot analysis

MoSUMO and sumoylated proteins were detected using anti-MoSUMO in *M. oryzae*. Lane 1-Purified MoSUMO protein, Lane 2-Purified GST-MoSUMO fusion protein, Lane 3- Total protein from Wild type mycelia grown in CM, Lane 4-Protein Marker.

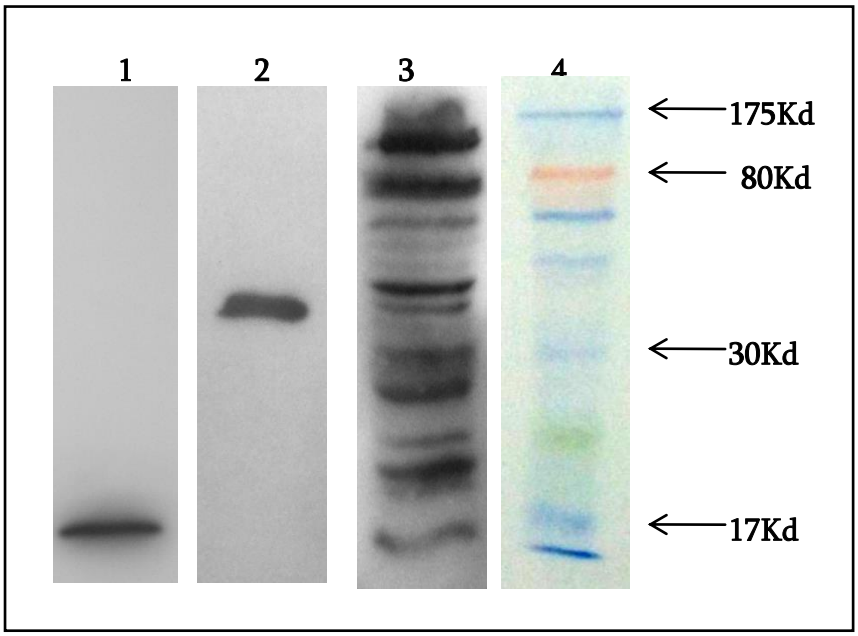
1
2
3
4
175Kd
80Kd
30Kd
17Kd

transformation. The resulting transformants were selected on zeocin and confirmed by Southern blot analysis. Briefly, genomic DNA of these transformants was digested with *Nco*I restriction enzyme and hybridized with 'probe a.' (5'flanking region of MoSUMO gene and GFP). Out of 11 transformants, one transformant showed single integration whereas multiple integrations were observed in rest of the transformants (Figure 20B). This was confirmed with different restriction enzymes and different probes. Genomic DNA of selected transformant and wild type were digested with *Eco*RI and hybridized with 'probe b' (MoSUMO and Zeocin gene). This was further confirmed with different restriction enzymes, probed with 'c' (GFP and MoSUMO gene). The hybridization pattern of Southern analysis confirmed the single integration of GFP::*MoSUMO* in genome of *M. oryzae*. The localization transformant was phenotypically similar to the wild type with respect to growth, conidiation, appressorial development and pathogenicity (Figure 21A,B,C).

4.12 Subcellular localization and live cell imaging of MoSUMO

The live cell imaging of MoSUMO localization transformant was carried out. A time course evaluation in terms of GFP signal was performed to track the localization of MoSUMO during the development of appressoria from conidia at 0hr, 2hr, 3hr, 4hr and 7hr. The GFP signal was detected throughout the conidium

(Figure 22, 0hr) which indicates that MoSUMO and/or sumoylated proteins were present throughout the conidium. As the time progressed, the GFP signal moved towards the pole of conidia (Figure 22, 2h,3h,4h) and finally intense GFP signal was seen in appressoria (Figure 22, 7h). These results suggested that abundance of MoSUMO and/or MoSUMO conjugates were present during developmental stages of appressoria. MoSUMO expression was also analyzed microscopically during the infection of rice leaf and observed that the invasive hyphae also showed the GFP signal indicating MoSUMO and/or sumoylated proteins were expressed during infection after 12hpi in host tissue (Figure 23).

Figure 19: Indirect immunolocalization of MoSUMO

Immunostaining was performed in vegetative hyphae (A) and conidia (B) of *M. oryzae*. TRITC conjugated secondary antibody was used to stain MoSUMO protein. Chitin staining was performed with CFW simultaneously. Bar-10μm.

A.

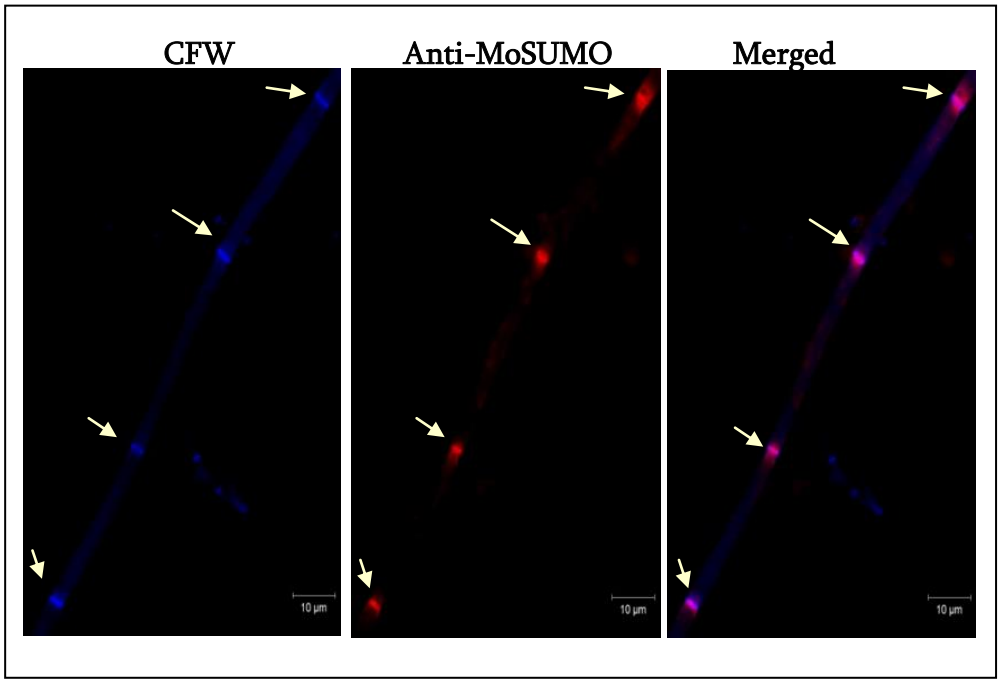
CFW
Anti-MoSUMO
Merged
10 µm
10 µm
10 µm

B.

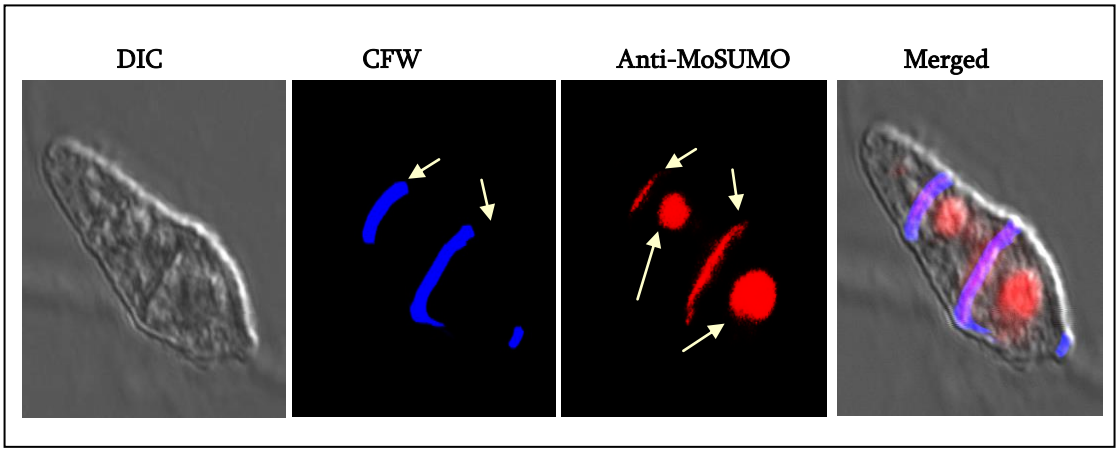
DIC
CFW
Anti-MoSUMO
Merged

Figure 20: Southern blot of GFP::MoSUMO transformants

A. Schematic representation of localization construct of MoSUMO.

B. Southern blot analysis of GFP::SUMO fusion transformants and Wild type (WT). Genomic DNA of both digested with *Nco*I and hybridized with a. probe. Lane1-11- Putative localization transformants. Lane 12 -WT and Lane 13- Marker. Transformant No.2 was showing single integration and rests of the transformants were having multiple integration.

C. Genomic DNA of selected transformant no. 2 and WT digested with *EcoR*I and hybridized with b.probe (Left Panel). This was further confirmed with different restriction enzymes including *Nco*I(N), *Nde*I(Nd) and *BamH*I(B) and hybridized using probe c (Right Panel).

A.

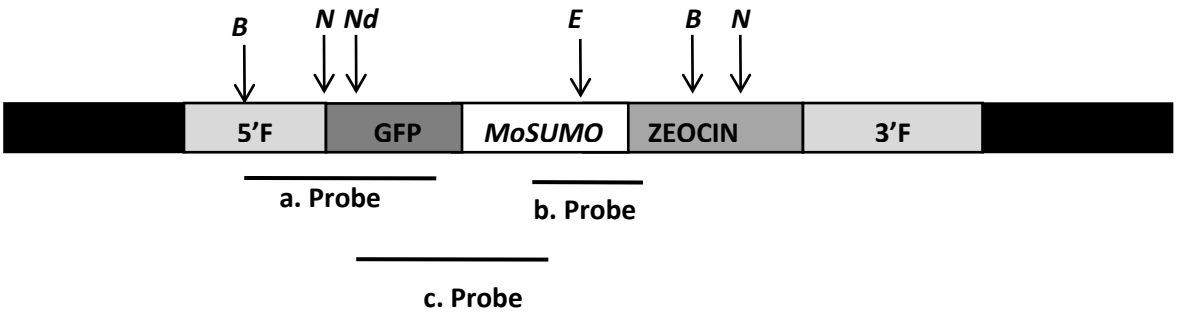
B
N Nd
E
B
N
5'F
GFP
MoSUMO
ZEOCIN
3'F
a. Probe
b. Probe
c. Probe

B.

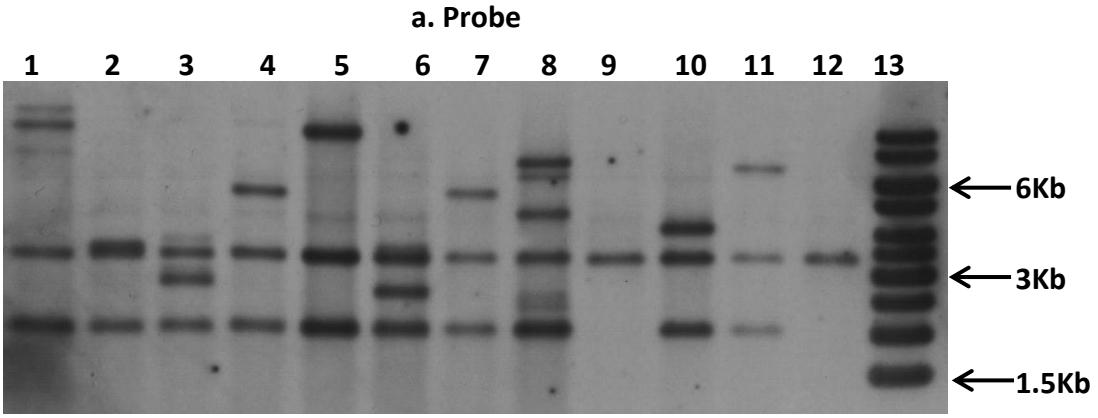
a. Probe
1 2 3 4 5 6 7 8 9 10 11 12 13
6Kb
3Kb
1.5Kb

C.

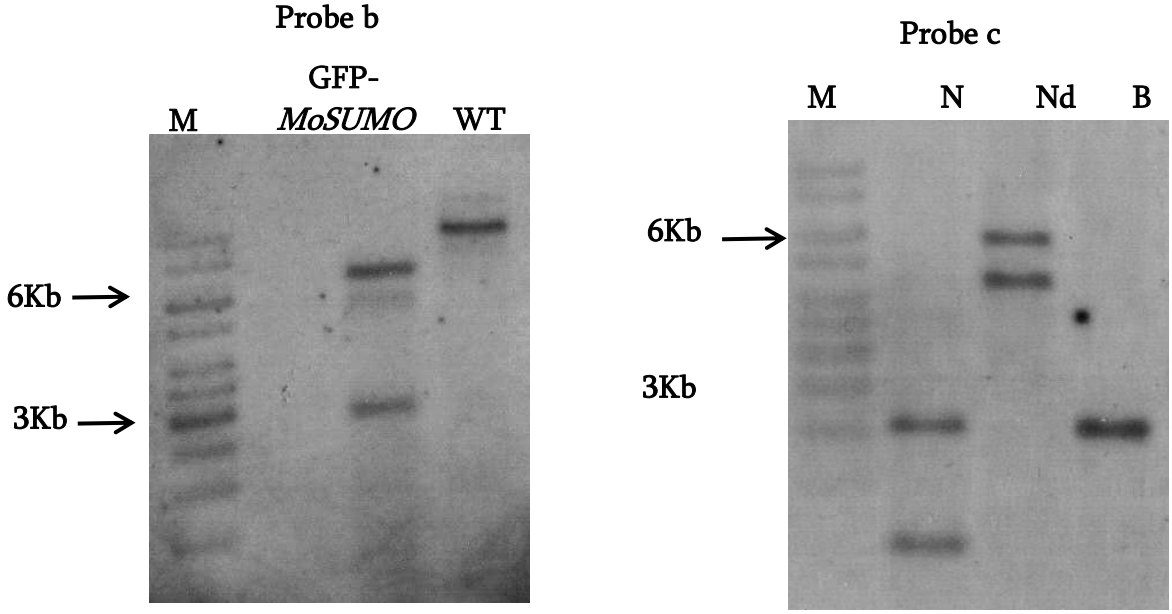
Probe b
GFP-
MoSUMO
M
WT
6Kb
3Kb
Probe c
M
N
Nd
B
6Kb
3Kb

4.13 Co-localization of MoSUMO at nuclear and septal regions

The vegetative hyphae were stained with DAPI and CFW to visualize the nuclei and chitin, respectively. The GFP fluorescence was observed at the nuclear region and also in the septal region. The above observations re-affirmed the previous indications that MoSUMO and/or sumoylated proteins were abundantly localized in nuclei and septal region of vegetative hyphae (Figure 24). *In silico* analysis of septins was performed using GROMO and SUMOsp databases and the result showed that septins were probable targets of MoSUMO protein (Table 2).

4.14 Co-localization of MoSUMO and actin protein

Since defective morphology was observed during development of appressoria from conidia in *ΔMosumo* mutant, attempts were made to check the cytoskeletal proteins as likely MoSUMO targets. The conidia of GFP::MoSUMO transformant were harvested from 7 days old culture and stained with rhodamine phalloidin. The confocal microscopic observation showed the overlapping of MoSUMO and actin fluorescent signals, indicating that actins might be the probable target of MoSUMO (Figure 25). *In silico* analysis was carried out using SUMOsp database. Sumoylation sites were predicted and it was found that Actin1 (MGG_03879) and Arp related protein 5 (MGG_06130) had sumoylation consensus sequences (Table 2).

Figure 21: Phenotype of GFP::MoSUMO transformant

A. Five day old culture of Wild type and GFP::MoSUMO strain grown on OMA showing growth and aerial hyphae.

B. Appressorial development of Wild type and GFP::MoSUMO strain after. Bar-10μm.

C. Drop inoculation assay of Wild type and GFP::SUMO strain on rice leaves after 4 dpi. Typical blast lesions were observed in both.

A.

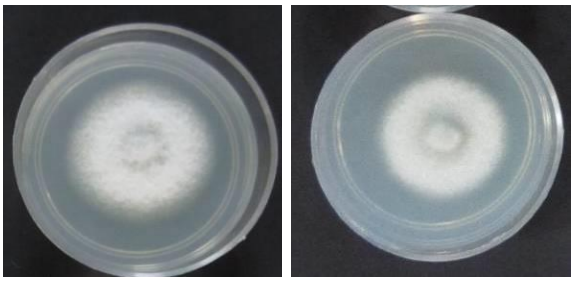

Wild type GFP::MoSUMO

B.

Wile type GFP::MoSUMO

C.

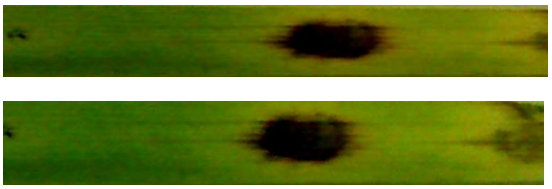

Wild type

GFP::MoSUMO

Figure 22: Subcellular localization of MoSUMO in developmental stages of appressoria

MoSUMO localization was monitored during developmental stages of appressoria. Time lapse live cell imaging of MoSUMO localization in conidia (0hr) up to the formation of appressoria (7hr) was examined using confocal laser microscope. Bar-10μm.

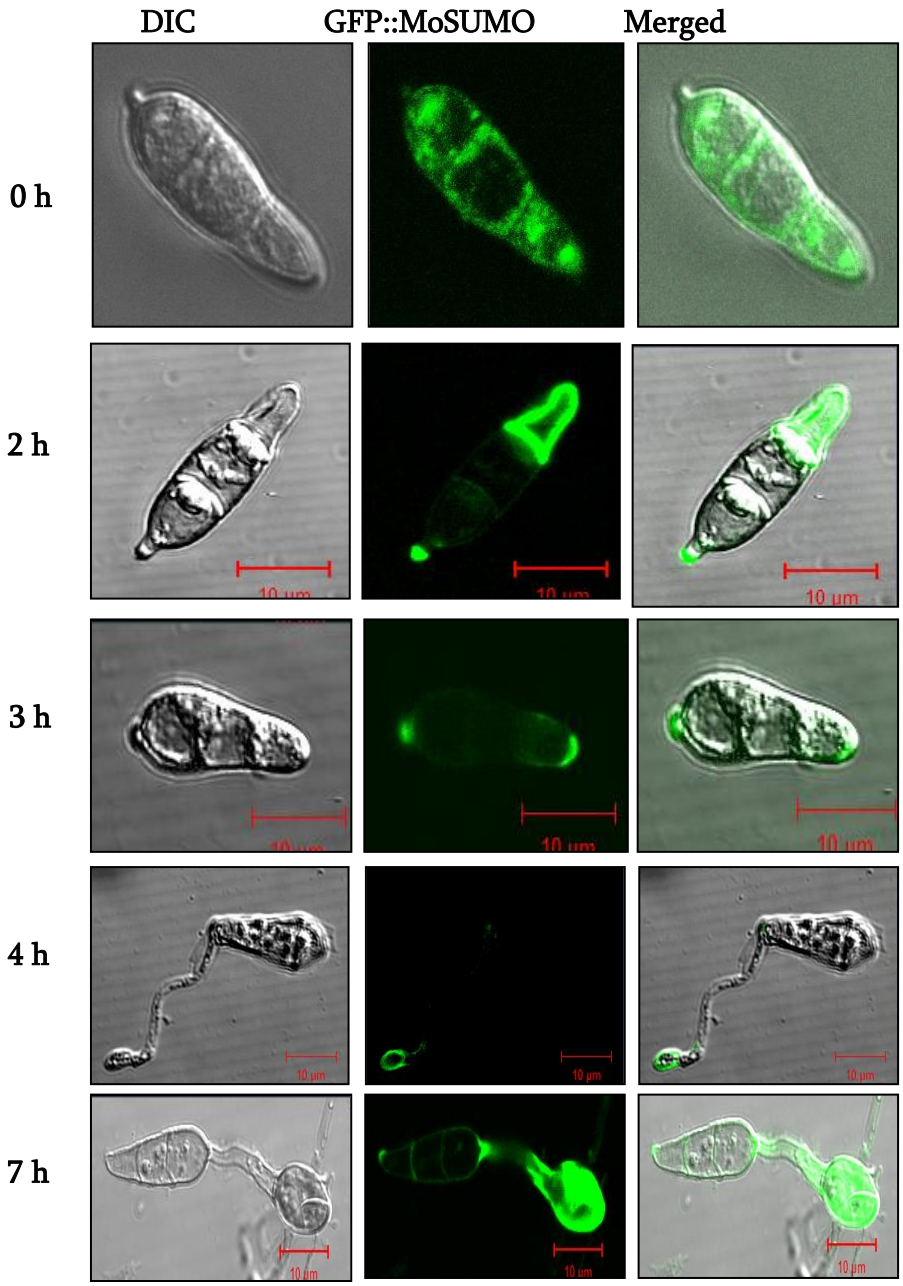
DIC
GFP::MoSUMO
Merged
0 h
2 h
3 h
4 h
7 h
10 µm

Figure 23: Localization of MoSUMO of *M. oryzae* in host tissue

The conidia of GFP::MoSUMO transformant were inoculated on leaf surface and examined after 12 hpi. MoSUMO expressed throughout the cell after entering the host tissue including conidia (C), appressoria (AP) and branched invasive hyphae (BIH). Bar-10μm.

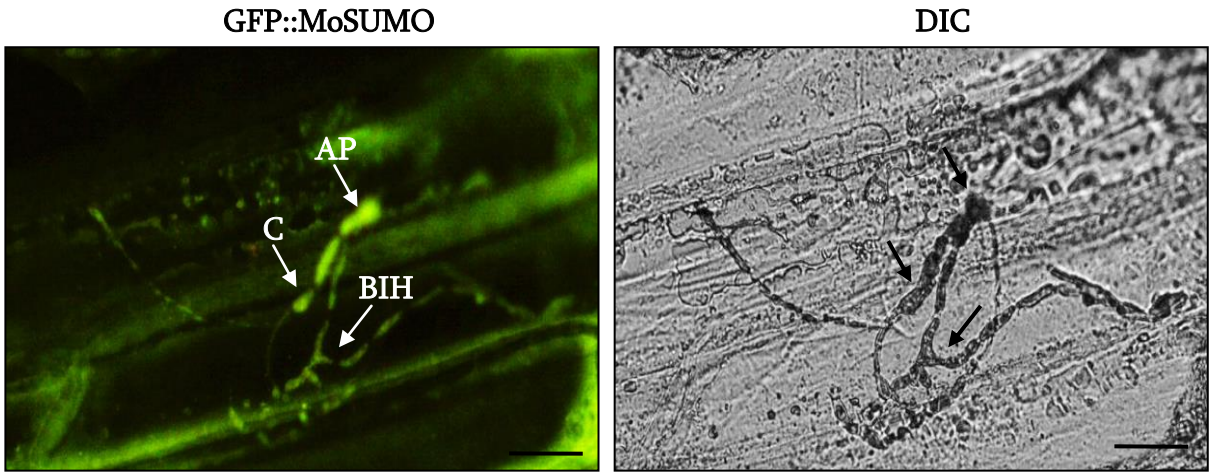
GFP::MoSUMO
DIC
AP
C
BIH

Figure 24: Colocalization of MoSUMO, at nuclear and septal region of hyphae

Hyphae were stained with DAPI and CFW. Upper panel-DIC, Nuclei and chitin staining (DAPI+CFW panel). GFP signals were observed at the corresponding sites of nuclei and septa (GFP panel) and the lowermost panel showing merged image of GFP-SUMO expression. Arrowheads pointed at septa and nuclei. N-Nucleus, S-septum, Bar-10μm.

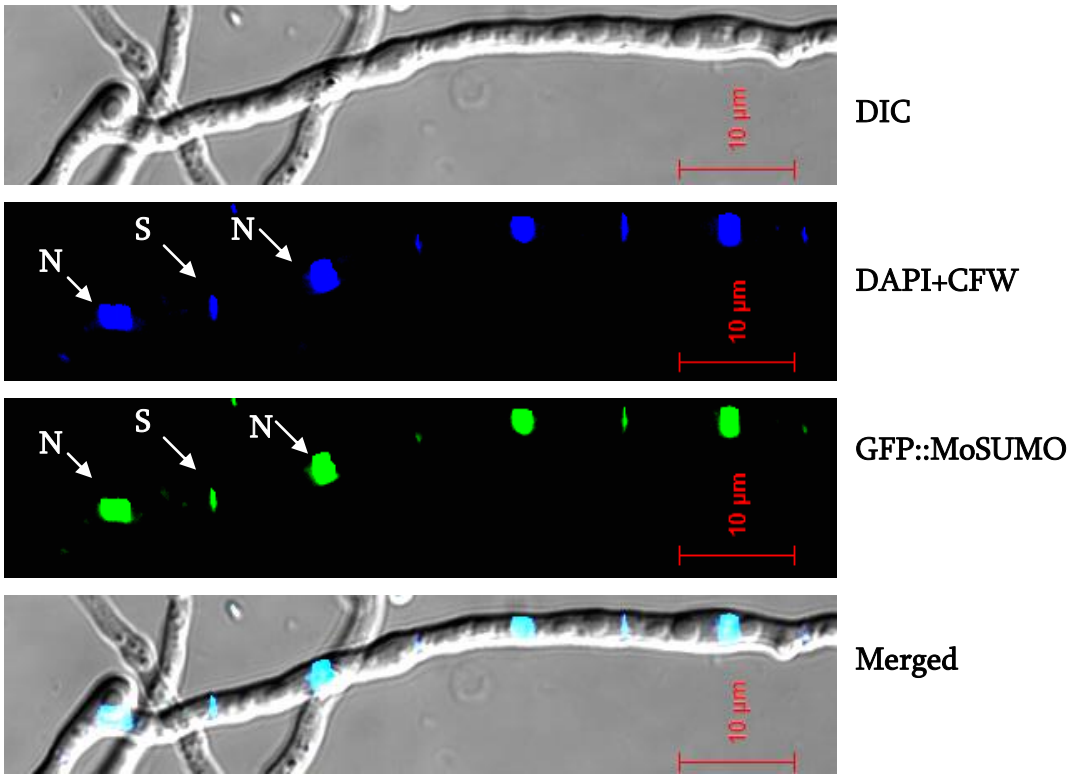
DIC
DAPI+CFW
GFP::MoSUMO
Merged
S
N
N
10 µm

Figure 25: Colocalization of MoSUMO and actin protein

The conidia of GFP::MoSUMO transformant were harvested from 7 days old culture and stained with rhodamine phalloidin. MoSUMO and actin localization was observed at the corresponding sites. Bar-10μm.

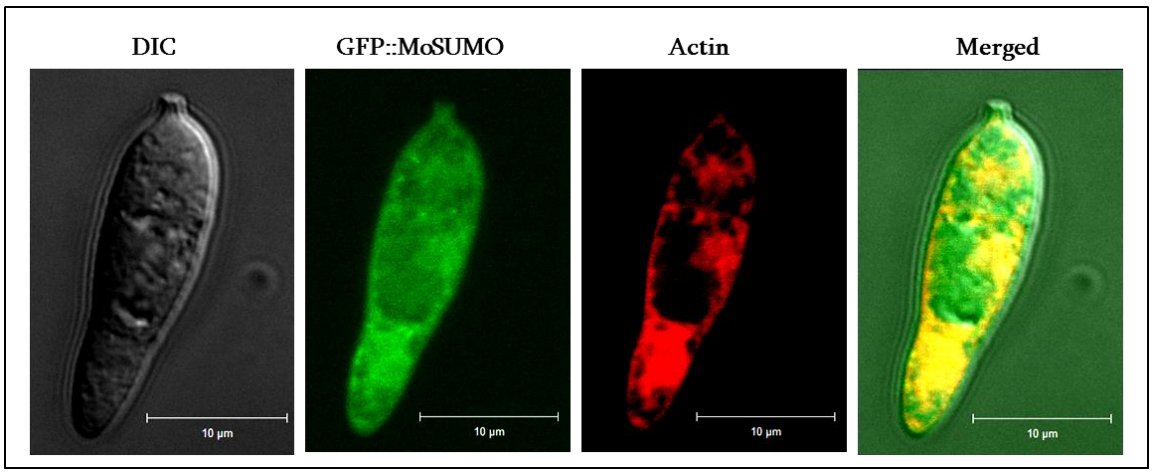
DIC
GFP::MoSUMO
Actin
Merged
10 µm
10 µm
10 µm
10 µm

Table 3. Prediction of sumoylation sites in septins, chitin synthases and actins of *M. oryzae* by software SUMOsp 2.0. The predicted sumoylation consensus site and SIM interaction sites (non-consensus sumoylation sites) are highlighted in red.

Gene ID	Function	Position	Peptide	Predicted Sumoylation Site
MGG_01521	Cell division control protein 3 (Sep3)	333 – 337 346 396	GRRYPWGVIEVDNEE HCDF EEHCDFVKLRQMLIR KEVNPAVKQEEERTL	SUMO Interaction Sumoylation Sumoylation
MGG_06726	Cell division control protein 10 (Sep10)	198 258-262	QAFKERIKEEFAFHN GRQNRWGVINVEDEE HCEF	Sumoylation SUMO Interaction
MGG_03087	Cell division control protein 11 (Sep11)	67 – 71 248 – 252 306 318	EGVKIKDITVELELDE DGT ARQYPWGVVEVDNP RHSDF AGVDSSMKPEDLASQ ASQSVRLKEEQLRRE	SUMO Interaction SUMO Interaction Sumoylation Sumoylation
MGG_07466	Cell division	240 248	IGSEKDVKTGDGRIV TGDGRIVKGRQYSWG	Sumoylation Sumoylation

	control protein 12 (Sep12)	318 333	KLDNPKFKEEEEALR KRFTEQVKIEEQRFR	Sumoylation Sumoylation
MGG_01802	Chitin Synthase (CHS1)	234 – 238 313 539 730 – 734 770-774 810-814	MYNRHTELLIAITYYN EDK IYQDGVVKKDVHGQE LSYIKAAKGETDVPE GKSGAAGVILLALIAIY GI MLLMSTYINILMVYAF NNW TKGEKDEVVVEEIDKP QED	SUMO Interaction Sumoylation Sumoylation SUMO Interaction SUMO Interaction SUMO Interaction
MGG_03879	Actin1	249 317 – 321	LKTAQEIKEEYCYVC DFLTPLPVVVDGVIQS SPI	Sumoylation SUMO Interaction
MGG_03982	Actin	94 – 98	VAPEEHPVLLTEAPIN PKS	SUMO Interaction
MGG_05587	Actin	63 – 67 392 – 396 421 – 425	SGGSKPNILRIPNCIAR DR WPGLLANIVVVGGNA LFDG QLVPDECIVRVARPFD PIT	SUMO Interaction SUMO Interaction SUMO Interaction
MGG_10690	Actin- 6	86 244 – 248	PMENGIVKKWDDMQ H RLSEDTTVLVESYTLP DGR	Sumoylation SUMO Interaction

MGG_06130	Actin-related protein 5	62 – 66 348 474	ATSQGGPVAIVIDNGS SAV MRLDRLVKKEQELEY QEAAARVKEREMLSK	SUMO Interaction Sumoylation Sumoylation
MGG_06064	Chitin Synthase (CHS1)	47 128 – 132 141 – 145 288 - 292	CLVKVFIKAEHWTIR DEVSAPKVVIVMPCY KEDP CYKEDPEVLLVAMNSI VDC TTKKHSLITVLQDLEYI HG	Sumoylation SUMO Interaction SUMO Interaction SUMO Interaction
MGG_04145	Chitin Synthase (CHS2)	542 737 - 741 748	GPLSQYFKGETLHGQ TTFAAFYIVIRQLTDPK AK QLTDPKAKLEMGNNV	Sumoylation SUMO Interaction Sumoylation

4.15 Global protein profiling of wild type B157 and *ΔMosumo* mutant

The investigation of differential protein expression of wild type and *ΔMosumo* mutant was achieved using proteomic approach. Two mg mycelial protein of wild type and *ΔMosumo* mutant was run on two dimensional gel electrophoresis (2DGE) in replicates. One set of gels were stained with Coomassie brilliant blue (Figure 26). Analysis was carried out using PD Quest software. Quantitative analysis (scatter plot) revealed that 72 protein spots were absent, 36 protein spots were up regulated and 56 spots were down regulated in *ΔMosumo* mutant (Figure 27).

4.16 Identification of isolated proteins from 2DGE by MALDI-TOF

Out of 72 spots which were absent, prominent four spots were picked up randomly. The peptide sequencing of differentially expressed protein spots from 2DGE was carried out using MALDI-TOF /TOF analysis. The masses obtained in the peptide mass fingerprint were submitted for FLEX software for identification of the protein. The chromatogram of identified spots were shown in figure 28A,B,C and D. These were designated as the abbreviation 'S' and sumoylation sites were predicted using GROMO and SUMOsp 2.0 database with high cut off value (Table 3).

4.17 Enrichment of sumoylated proteins of *M. oryzae*

Enrichment of sumoylated proteins was attained using SUMO qapture-T kit according to manufacturer's instructions. This method facilitates the purification of low abundance sumoylated proteins from total protein extracts. Optimization of the binding for sumoylated proteins was carried out using sumoylated protein lysate, supplied with kit and GST-MoSUMO fusion protein (Figure 29A). Total mycelial proteins of wild type were used for the enrichment of sumoylated proteins. Captured proteins were eluted under denaturing conditions followed by western blot analysis, using the MoSUMO specific antibody. Result indicated that large numbers of protein were getting sumoylated at the mycelia stage (Figure 29B).

Figure 26: Two dimensional gel electrophoresis of Wild type and *ΔMosumo* mutant

A representative coomassie brilliant blue stained gel of fungal mycelia from Wild type and *ΔMosumo* mutant. Proteins were separated by isoelectric focusing on 3 to 10 nonlinear immobilized pH gradient strips for the first dimension and second dimension was run on 12% linear polyacrylamide gel. PDQuest 2-D analysis Software 8.0 (Advance) was used the differential protein expression. The positions of PAGE molecular mass markers are shown in kilodaltons on the right of the gel image. The marked (Red) spots were chosen for further analysis.

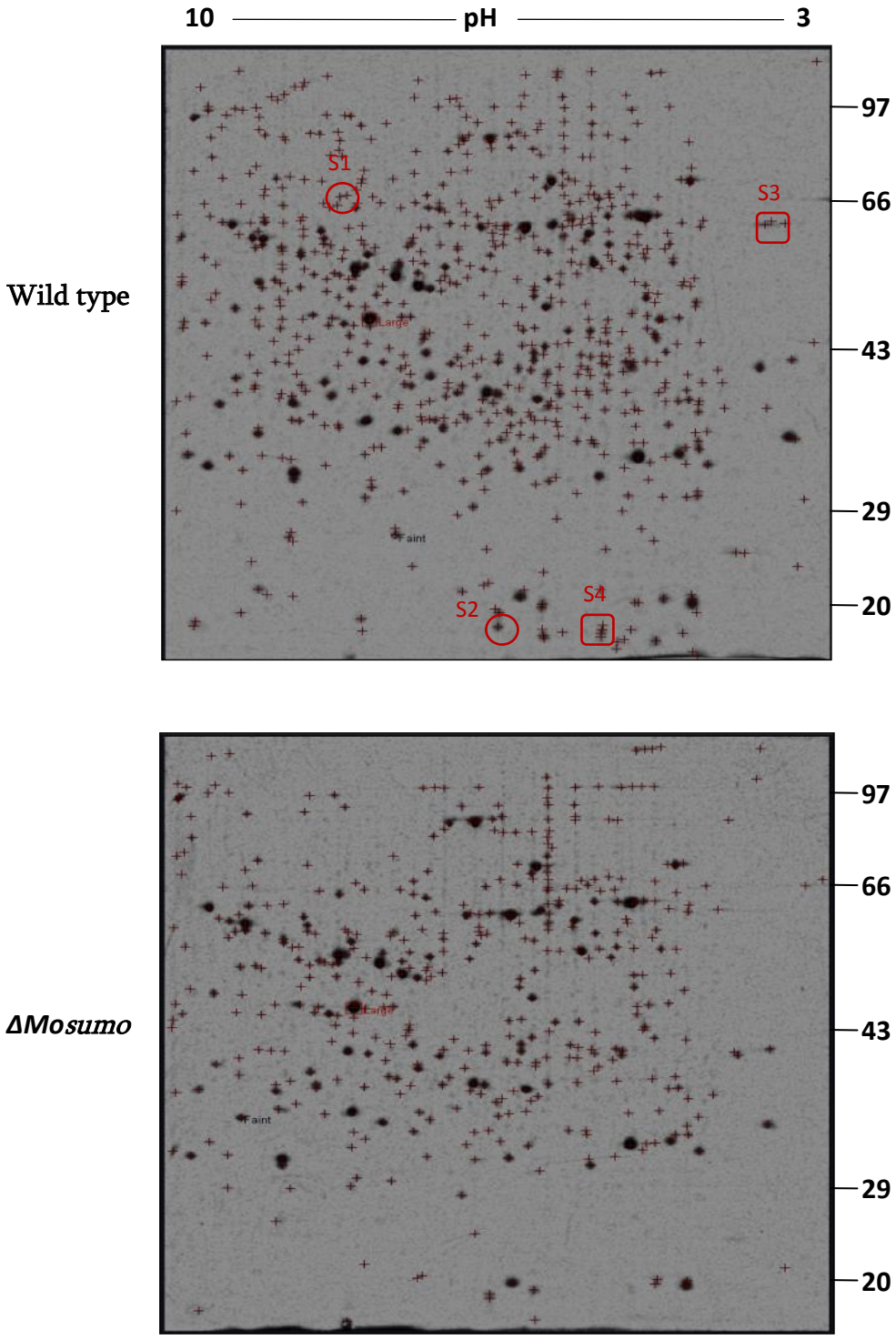
10
pH
3
Wild type
S1
S2
S3
S4
97
66
43
29
20
ΔMosumo
97
66
43
29
20

Figure 27: Scatter plot analysis of 2DGE of WT versus *ΔMosumo* mutant

Quantitative analysis of 2DGE was carried out using PD Quest software and scatter plot revealed that 72 protein spots were absent, 36 protein spots were up regulated and 56 spots were down regulated in *ΔMosumo* mutant.

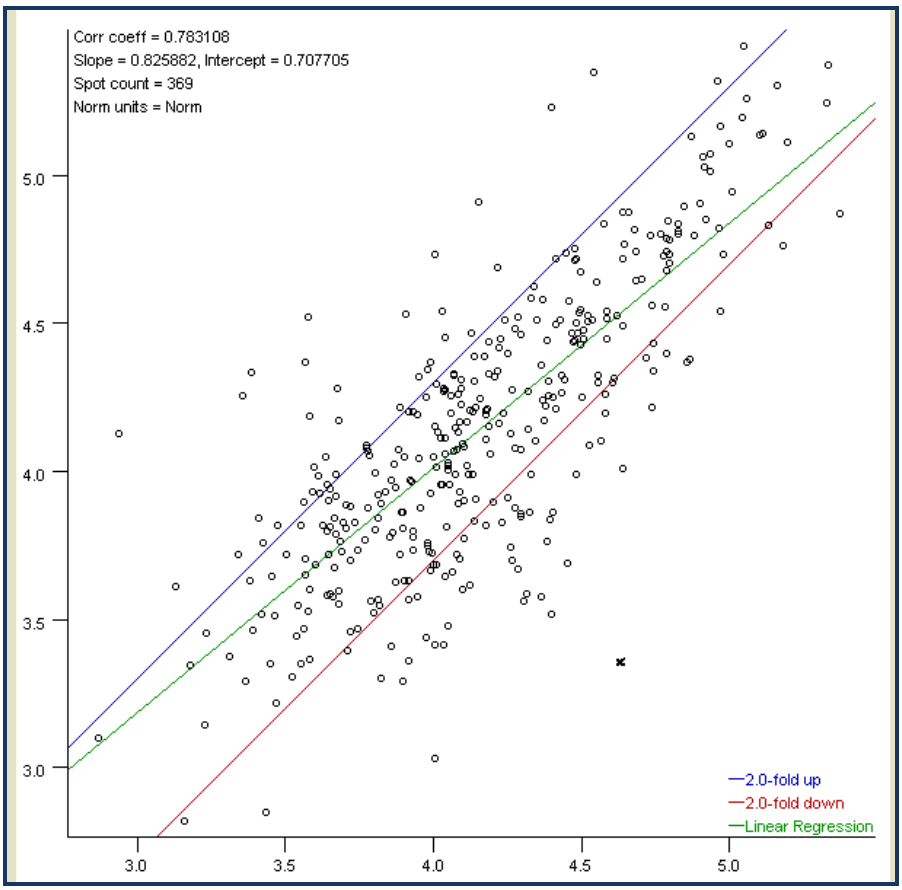
Corr coeff = 0.783108
Slope = 0.825882, Intercept = 0.707705
Spot count = 369
Norm units = Norm
5.0
4.5
4.0
3.5
3.0
3.0
3.5
4.0
4.5
5.0
2.0-fold up
2.0-fold down
Linear Regression

Figure 28: Chromatogram of identified protein spots using MALDI-TOF/TOF and detail of peptide mass fingerprinting

A. Spot S1. MGG_06958.6 - HSP70 like protein

B. Spot S 2. MGG_14792.6-Mitochondrial ribosomal protein subunit S18

C. Spot S 3. MGG_16530.6 - Conserved hypothetical protein

D. Spot S4. MGG_10292.6 - Conserved hypothetical protein

A

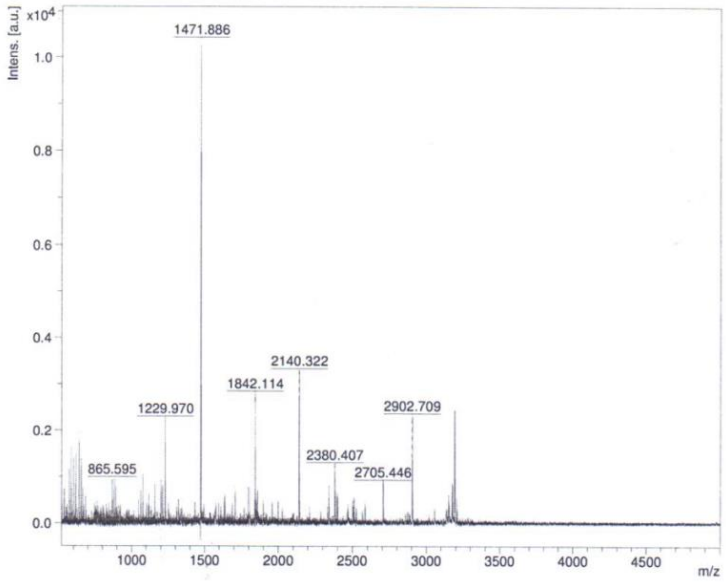

m/z	S/N	Quality Fac.	Res.	Intens.	Area
539.063	6.3	2386	3891	723.54	152
569.197	9.7	2520	2652	1117.80	364
584.414	14.6	5860	3528	1705.84	436
599.783	10.9	1431	3530	1272.24	330
615.418	13.3	4458	4508	1555.26	342
637.392	15.8	5139	4749	1855.77	410
653.368	12.6	1974	4654	1467.78	339
865.595	7.0	216	4697	818.55	274
881.348	6.0	347	3291	703.61	338
1061.624	6.1	893	6262	698.87	243
1077.323	6.3	286	3312	717.03	467
1158.784	7.8	773	5752	869.38	365
1200.791	8.6	2892	5953	950.24	415
1229.970	20.7	5477	5164	2248.17	1192
1471.886	100.6	108987	6917	10383.33	5698
1842.114	27.9	28141	6616	2600.58	2317
2140.322	34.6	30860	7029	2630.68	2657
2340.626	6.8	871	3188	424.85	1039
2380.407	13.0	1310	5753	807.70	1133
2384.259	6.0	1218	4948	372.69	624
2397.414	6.2	282	4236	383.70	733
2509.539	7.0	548	5721	398.04	611
2705.446	9.9	2212	6470	494.16	755
2902.709	32.5	10655	6979	1397.42	2211
3150.541	7.0	300	2115	177.65	1100
3174.991	14.4	2092	5577	501.90	1175
3189.946	38.7	8345	6910	1345.62	2569
3205.927	7.6	1028	6774	260.46	503

B

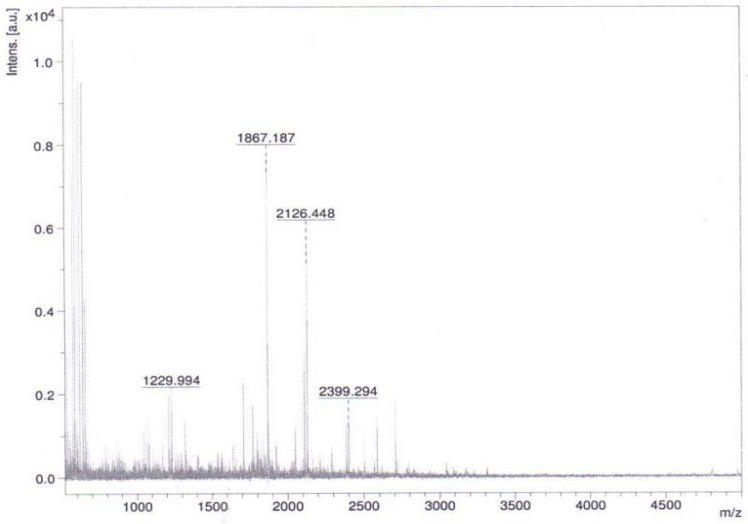

m/z	S/N	Quality Fac.	Res.	Intens.	Area
534.335	17.6	1286	1222	2643.36	1707
539.071	10.6	378	2654	1593.01	475
566.450	7.5	159	1958	1107.51	476
569.208	44.4	9667	2394	6592.40	2350
584.432	67.4	10045	2950	9959.26	2994
599.812	62.9	19274	3873	9315.18	2238
615.446	67.0	4779	4415	9920.19	2247
637.417	68.0	9657	4400	9979.91	2360
653.388	39.2	2822	4554	5759.14	1363
1061.630	9.8	1294	4594	1261.15	584
1076.739	6.5	323	5773	828.34	330
1077.328	8.8	303	3556	1125.79	681
1211.902	15.1	1370	5127	1882.11	976
1229.994	17.0	1812	5351	2118.08	1069
1320.773	10.6	2162	5461	1294.05	736
1707.986	17.7	7152	6087	1986.10	1631
1767.239	13.9	2566	6216	1542.28	1309
1798.055	8.8	1681	6537	959.92	814
1839.137	8.3	3667	8902	892.83	585
1867.187	68.5	37558	7117	7330.08	6198
1869.228	12.5	551	6438	1333.22	1216
1922.273	6.4	436	4581	650.46	872
2048.269	10.6	2965	7309	959.97	873
2109.420	27.5	9946	6738	2354.55	2422
2126.448	60.6	76289	8199	5111.31	4378
2286.389	6.0	1411	5607	437.91	598
2384.243	13.8	1163	5486	899.29	1339
2399.294	18.2	2078	6354	1176.44	1521
2501.509	11.7	2367	6699	688.76	893
2584.502	16.5	3108	7110	895.35	1156
2705.473	24.3	5671	7752	1175.70	1502

C

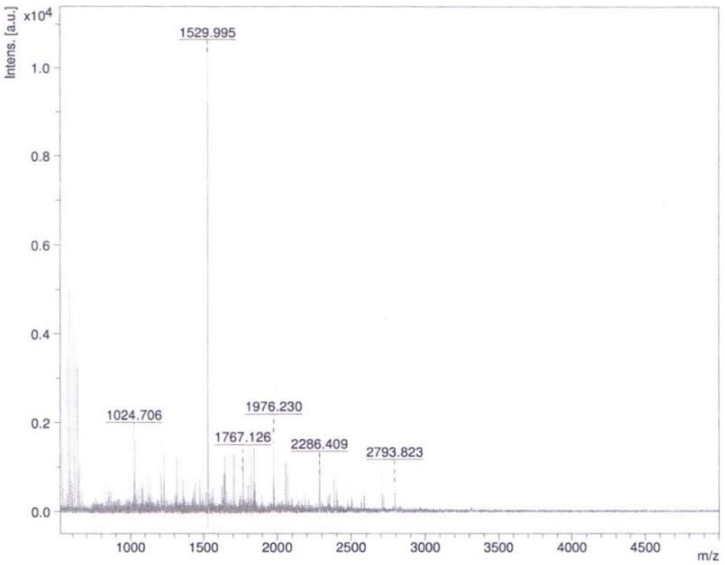

m/z	S/N	Quality Fac.	Res.	Intens.	Area
534.325	14.7	1625	1254	1312.39	828
566.450	7.7	187	1892	687.13	307
569.216	35.4	15999	2380	3168.22	1147
581.816	7.1	194	2032	634.31	272
584.426	52.4	4239	2929	4715.31	1421
597.433	7.0	193	3804	636.50	157
599.809	47.1	10550	3928	4307.84	1031
615.459	48.6	4185	4387	4467.45	1010
637.419	36.6	6556	3783	3348.05	907
653.388	12.6	591	3098	1159.91	387
831.530	18.1	3520	4927	1723.27	533
865.628	7.7	263	4926	737.04	239
1024.706	19.6	13424	5566	1946.23	722
1032.708	16.0	18731	5443	1582.11	603
1061.639	7.4	587	5385	724.60	293
1077.349	7.0	245	3067	689.69	484
1085.799	6.4	1121	5445	634.86	262
1119.746	7.4	1308	4653	727.44	363
1136.733	6.1	572	3845	601.50	367
1229.998	14.8	1566	4391	1461.21	901
1320.810	10.8	1286	3929	1064.62	833
1444.875	8.3	2697	6483	811.21	449
1475.951	6.1	1406	5481	596.15	410
1529.995	107.3	35698	6016	10337.30	6931
1562.003	8.9	811	4474	853.82	796
1639.056	7.9	918	5263	740.08	643
1645.955	12.4	2268	5501	1161.62	979
1707.992	12.7	11955	6571	1175.05	901
1767.126	10.0	989	4526	907.39	1065
1823.139	13.4	8392	6518	1190.30	1045
1844.273	15.4	7122	6810	1361.40	1161
1976.230	22.5	11395	6243	1772.33	1821
2057.309	12.8	3593	6300	933.75	1000
2071.293	8.1	845	5054	583.45	770
2283.422	8.8	738	6114	514.67	649
2286.409	14.3	2507	6503	830.76	984
2384.231	11.4	1105	5562	593.93	864
2399.299	8.5	1311	6010	435.34	594
2501.512	10.0	928	5565	462.19	719

D

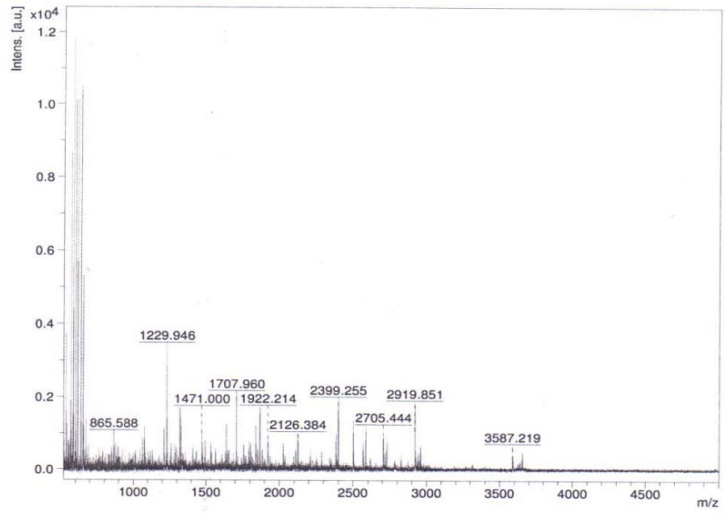

m/z	S/N	Quality Fac.	Res.	Intens.	Area
534.350	20.5	2269	1168	3265.02	2222
564.965	6.1	1019	3973	970.49	215
566.444	8.9	373	1864	1404.57	638
569.208	50.1	13833	2330	7956.44	2940
581.808	6.3	82	1477	991.73	580
584.417	68.9	8640	2708	10891.05	3551
599.793	61.4	14506	3633	9758.91	2495
615.427	65.9	8206	4333	10473.74	2396
637.403	66.8	25590	3920	10444.74	2697
653.371	33.8	4461	4065	5266.16	1349
672.041	6.1	276	2503	945.72	402
865.588	7.2	276	4205	1033.45	382
1076.721	6.4	622	5150	858.45	385
1211.880	6.9	203	3065	876.39	750
1229.946	27.3	5936	5082	3451.45	1855
1320.747	12.5	2852	5059	1552.47	945
1325.861	12.3	5290	6607	1516.35	723
1471.000	8.5	6405	7000	1003.90	530
1493.904	6.3	2208	6977	750.73	418
1532.984	6.3	3922	6794	732.31	432
1639.018	10.9	4402	6541	1217.20	858
1707.960	17.1	10957	5765	1881.02	1635
1839.094	9.3	1630	5793	965.95	960
1867.154	14.2	6858	6321	1462.16	1385
1922.214	6.2	828	5163	610.14	724
2126.384	7.9	766	5386	653.72	835
2384.208	9.1	1468	5327	593.88	927
2399.255	20.4	9940	6722	1322.33	1626
2501.481	15.0	6326	6588	899.46	1199
2566.516	7.7	847	5997	439.49	659
2584.459	14.3	6677	7352	802.23	1008
2705.444	9.7	1118	5521	487.33	865
2727.493	9.3	1816	6538	458.56	696
2919.851	24.6	6199	7177	1052.67	1650
2941.791	6.2	1605	7161	262.37	420
2957.756	9.4	2352	7914	392.98	571
3587.219	10.6	2134	7492	279.61	593
3654.360	8.5	1268	7881	209.88	443

Table 4: Identity of the 2DGE differentially expressed protein spots as obtained by sequencing with MALDI-TOF/TOF and FLEX analysis software was used to obtain peptide mass fingerprint data. Sumoylation sites are predicted using GROMO and SUMOsp 2.0 databse with high cut off value. The predicted sumoylation consensus site and SIM interaction sites (non-consensus sumoylation sites) are highlighted.

Spot No. (Gene ID)	Score	Function	Position	Peptide	Predicted Sumoylation Site
S1 (MGG_06958)	66%	Hsp70-like protein	24 - 28 106 525	GIFRDDRIEIIAND QGN PVIEVEFKGESKQF LAEAEKFKEEDE	SUMO Interaction Sumoylation Sumoylation
S2 (MGG_14729)	51%	Mitochondrial ribosomal protein subunit S18	183 231	KINKLEV TRSKKPR	Sumoylation Sumoylation
S3 (MGG_16530)	45%	Conserved hypothetical protein	119 244	TLIASKWKHESAT SVDEAGVKNEQ	Sumoylation Sumoylation
S4 (MGG_10292)	71%	Conserved hypothetical protein	65 - 69 69	WTFKDGTVLDVK QEE DGTVLDVKQEE	SUMO Interaction Sumoylation

Figure 29: Western blot analysis of enriched sumoylated proteins in *M. oryzae*

A. Optimization of isolation of sumoylated proteins with control protein provided with kit and GST-MoSUMO fusion protein expressed in *E. coli,* using SUMO qapture-T kit. Proteins were run on 12% SDS-PAGE and western blotting was carried out using raised anti-MoSUMO antibody as a probe. Lane 1-Control sumoylated protein lysate provided with kit, Lane 2- Prestained protein marker, Lane 3-Bacterial protein lysate, Lane 4- Unbound fraction, Lane 5- Washed protein, Lane 6- Elute.

B. Detection of enriched sumoylated proteins from mycelial biomass of Wild type (WT) grown in CM for 3 days using anti-MoSUMO antibody. Lane 1- Prestained protein marker, Lane 2- Ponceau staining of proteins, Lane 3- WT total mycelial proteins.

A.

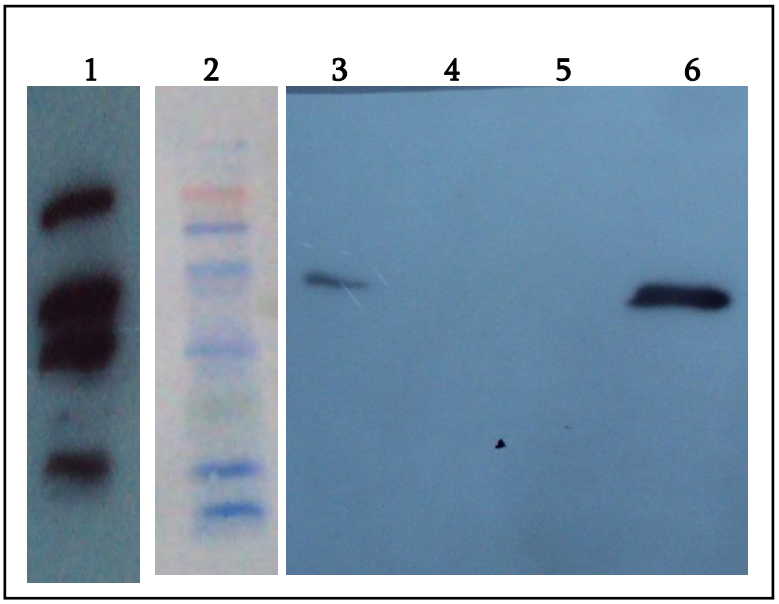

B.